Geoscience Frontiers 4 (2013) 481–502

Contents lists available at SciVerse ScienceDirect

China University of Geosciences (Beijing)

Geoscience Frontiers

journal homepage: www.elsevier.com/locate/gsf

Review

Two stages of immiscible liquid separation in the formation of Panzhihua-type Fe-Ti-V oxide deposits, SW China

Mei-Fu Zhou [a,*], Wei Terry Chen [a], Christina Yan Wang [b], Stephen A. Prevec [c], Patricia Pingping Liu [a], Geoffrey H. Howarth [c]

[a] Department of Earth Sciences, The University of Hong Kong, Hong Kong, China
[b] Key Laboratory of Mineralogy and Metallogeny, Guangzhou Institute of Geochemistry, Chinese Academy of Sciences, Guangzhou 510460, China
[c] Department of Geology, Rhodes University, P.O. Box 94, Grahamstown 6140, South Africa

ARTICLE INFO

Article history:
Received 5 October 2012
Received in revised form
27 March 2013
Accepted 30 April 2013
Available online 21 May 2013

Keywords:
Fe-Ti oxide
Gabbroic layered intrusion
Immiscible Fe-Ti-(P) rich melt
Emeishan Large Igneous Province
SW China

ABSTRACT

Magmatic oxide deposits in the ~260 Ma Emeishan Large Igneous Province (ELIP), SW China and northern Vietnam, are important sources of Fe, Ti and V. Some giant magmatic Fe-Ti-V oxide deposits, such as the Panzhihua, Hongge, and Baima deposits, are well described in the literature and are hosted in layered mafic-ultramafic intrusions in the Panxi region, the central ELIP. The same type of ELIP-related deposits also occur far to the south and include the Anyi deposit, about 130 km south of Panzhihua, and the Mianhuadi deposit in the Red River fault zone. The Anyi deposit is relatively small but is similarly hosted in a layered mafic intrusion. The Mianhuadi deposit has a zircon U-Pb age of ~260 Ma and is thus contemporaneous with the ELIP. This deposit was variably metamorphosed during the Indosinian orogeny and Red River faulting. Compositionally, magnetite of the Mianhuadi deposit contains smaller amounts of Ti and V than that of the other deposits, possibly attributable to the later metamorphism. The distribution of the oxide ore deposits is not related to the domal structure of the ELIP. One major feature of all the oxide deposits in the ELIP is the spatial association of oxide-bearing gabbroic intrusions, syenitic plutons and high-Ti flood basalts. Thus, we propose that magmas from a mantle plume were emplaced into a shallow magma chamber where they were evolved into a field of liquid immiscibility to form two silicate liquids, one with an extremely Fe-Ti-rich gabbroic composition and the other syenitic. An immiscible Fe-Ti-(P) oxide melt may then separate from the mafic magmas to form oxide deposits. The parental magmas from which these deposits formed were likely Fe-Ti-rich picritic in composition and were derived from enriched asthenospheric mantle at a greater depth than the magmas that produced sulfide-bearing intrusions of the ELIP.

1. Introduction

Several magmatic Fe-Ti-V oxide deposits in the Panzhihua-Xichang (Panxi) region, SW China, are hosted in layered mafic-ultramafic intrusions of the Emeishan Large Igneous Province (ELIP) (Fig. 1) (Zhong et al., 2002, 2003, 2005; Zhou et al., 2002a, 2005, 2008; Pang et al., 2008a,b, 2009, 2010; Shellnutt et al., 2009a; Bai et al., 2012). Examples are the giant Panzhihua, Hongge and Baima deposits (Ma et al., 2003). The Hongge deposit alone contains 4572 Mt of ore reserves with 1830 Mt of Fe, 196 Mt of Ti and 14.7 Mt of V (Yao et al., 1993). In addition to these three giant deposits, other deposits currently being mined include the Taihe deposit to the north of the Baima deposit (Fig. 1). Flood basalts of the ELIP cover an area of at least half a million square kilometers, but to date, related oxide deposits are only known in the Panxi region, which is located in the inner part of the ELIP (He et al., 2003, 2010; Xu et al., 2004). Two newly mined deposits, Anyi and Mianhuadi, are not well known from the literature. The Anyi deposit in Yunnan Province is about 130 km south of Panzhihua. The Mianhuadi deposit occurs in the Red River fault zone near the border of China and Vietnam. The

* Corresponding author. Tel.: +852 2857 8251.
E-mail address: mfzhou@hku.hk (M.-F. Zhou).

Peer-review under responsibility of China University of Geosciences (Beijing)

Production and hosting by Elsevier

1674-9871/$ – see front matter © 2013, China University of Geosciences (Beijing) and Peking University. Production and hosting by Elsevier B.V. All rights reserved.
http://dx.doi.org/10.1016/j.gsf.2013.04.006

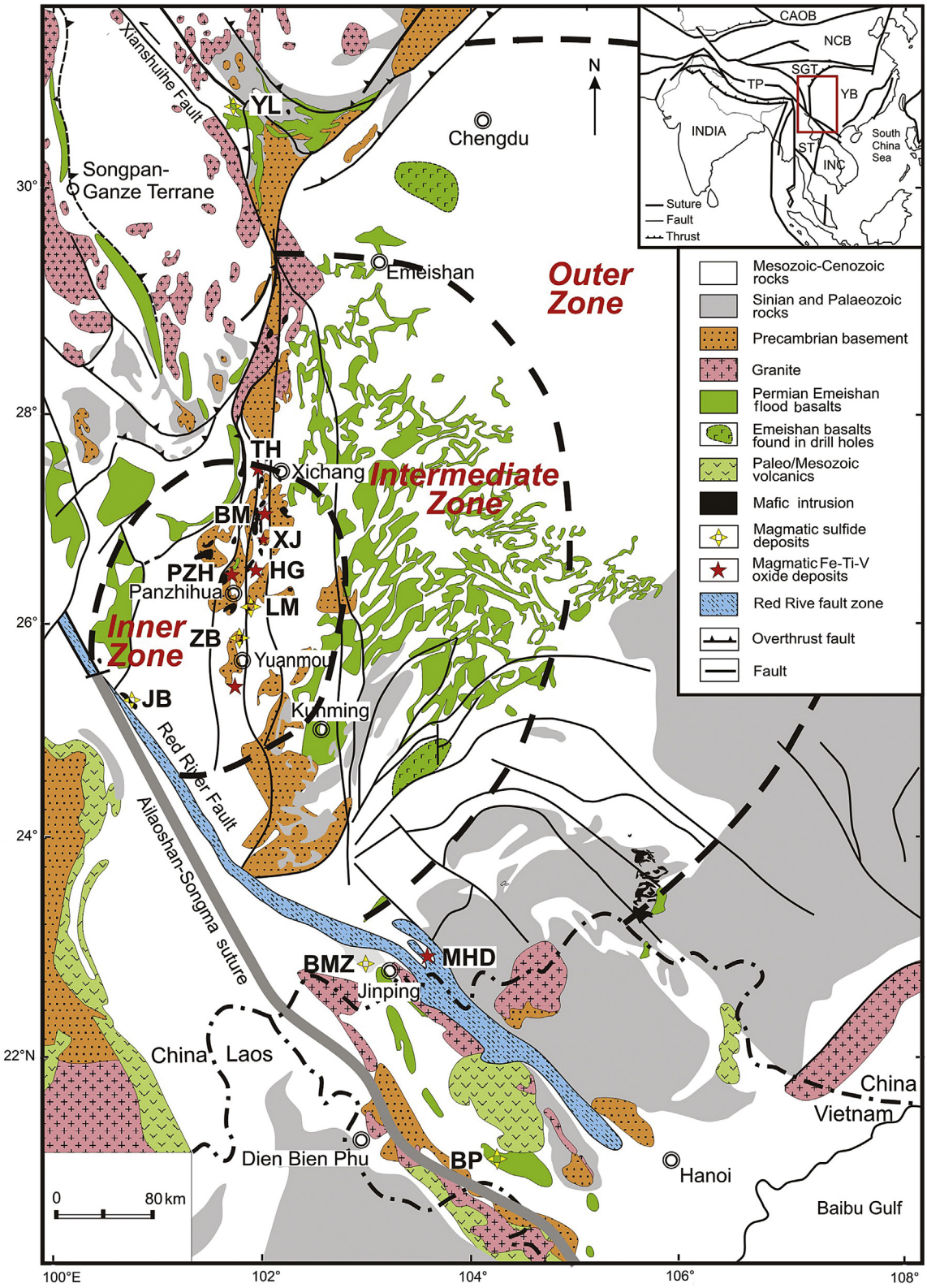

Figure 1. A simplified geological map of SW China and Northern Vietnam (modified from Wang et al., 2007) showing the distribution of the Emeishan Large Igneous Province (ELIP). Major blocks shown in the inset are: CAOB, Central Asia Orogenic Belt; NCB, North China Block; YB, Yangtze Block; INC, Indochina Block; TP, Tibetan Plateau; SGT, Songpan-Ganze Terrane; ST, Simao Terrane. Abbreviations of deposits: YL, Yangliuping; TH, Taihe; BM, Baima; XJ, Xinjie; HG, Hongge; PZH, Panzhihua; LM, Limahe; ZB, Zhubu; JB, Jinbaoshan; BMZ, Baimazhai; MHD, Mianhuadi; BP, Ban Phuc.

occurrence of oxide deposits away from the Panxi region may have significant implications for the ore genesis in relation to the mantle plume structure and also for exploration for the same type of deposits in the ELIP and elsewhere.

In the past few years, the giant Panzhihua and Hongge deposits have been the focus of many studies (Zhong et al., 2002, 2003, 2005, 2011; Zhou et al., 2005, 2008; Pang et al., 2008a,b, 2009, 2010; Bai et al., 2012; Ganino et al., 2013). These studies demonstrate that these deposits are different from oxide deposits hosted in larger layered gabbroic intrusions worldwide, such as the thin and laterally extensive magnetite layers in the Bushveld Complex, South Africa and the Sept Iles mafic intrusion, Canada (Cawthorn and Molyneux, 1986; Lee, 1996; Higgins, 2005). The mechanisms by which such large amounts of Fe-Ti oxides accumulated in the layered intrusions in the Panxi region is still a matter of debate. On the basis of the field relationships and petrography of oxide ores, Zhou et al. (2005) proposed a model involving the separation of immiscible oxide liquids from gabbroic magmas, in contrast to the more conventional model involving the settling and sorting of early cumulus Fe-Ti oxides (Pang et al., 2008a,b).

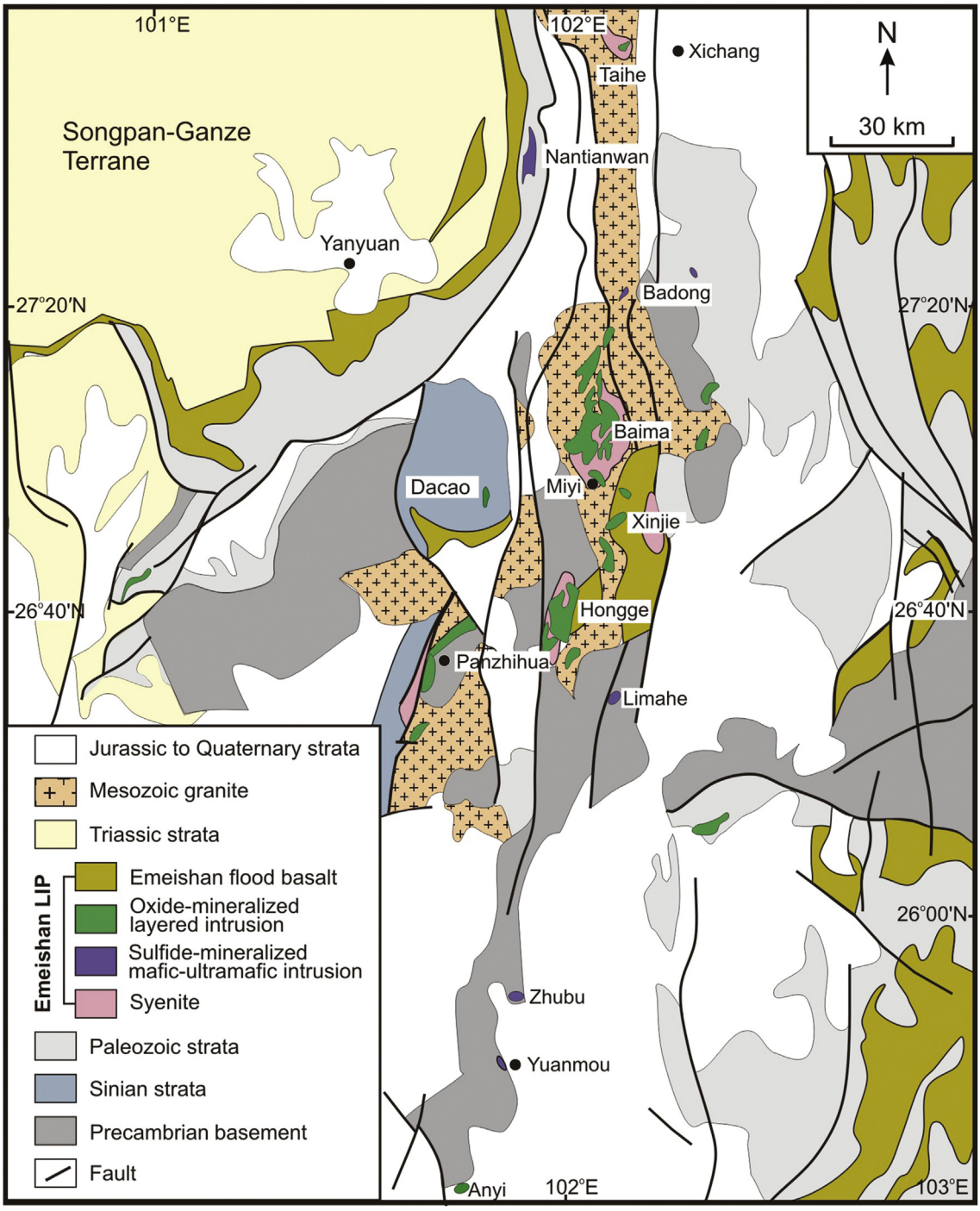

Figure 2. Distribution of the major Fe-Ti-V oxide deposits in the Panxi region (after Pang et al., 2008a). Note that the close association of oxide-bearing mafic-ultramafic intrusions and syenitic plutons.

In this paper, we review the available literature about these unique deposits which can be termed the Panzhihua type. Both the Anyi and Mianhuadi deposits are introduced and are used to demonstrate that oxide deposits of the ELIP are not restricted to the Panxi area. The close association of oxide ore-bearing mafic-ultramafic intrusions, syenitic plutons, and high-Ti flood basalts is emphasized. On the basis of all available data, we refine our previous model in which oxide ores formed from immiscible Fe-Ti-(P) rich melts in an evolved silicate magma.

2. Geology of the Emeishan Large Igneous Province

The Permian ELIP is located in the western part of the Yangtze Block and the eastern part of the Tibetan Plateau (Chung and Jahn, 1995) (Fig. 1). To the southeast, the ELIP occurs south of the Red River fault and extends to northern Vietnam.

The ELIP is composed dominantly of volcanic rocks with numerous mafic-ultramafic intrusions. A large number of papers dealing with the ELIP have been published (Chung and Jahn, 1995; Song et al., 2001; Xu et al., 2001; Ali et al., 2005; Shellnutt et al., 2010a and references therein). The flood basalts are believed to have been derived from a mantle plume at ~260 Ma (Chung et al., 1998; Xu et al., 2001, 2004; He et al., 2003, 2007, 2010). The volcanic succession is up to ~5 km thick and comprises low-Ti and high-Ti flood basalts, and picrites (Song et al., 2001; Xu et al., 2001; Hanski et al., 2004, 2010). There are also minor amounts of andesite and rhyolite in the sequence. This volcanic succession is underlain by the middle Permian Maokou limestone and overlain by shales and

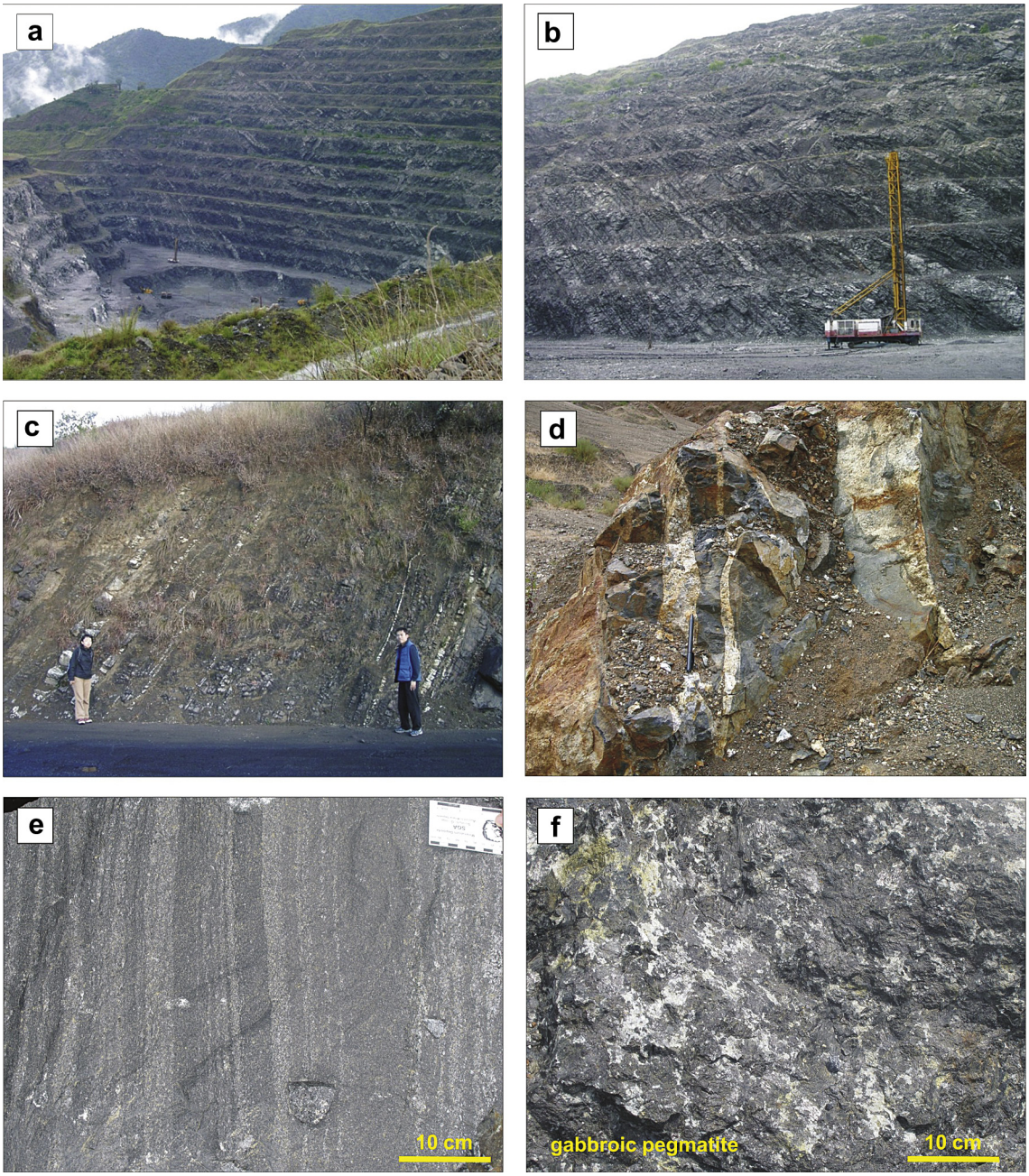

Figure 3. Magmatic layering of the oxide-bearing mafic intrusions in the Panxi region. a), b) and c) Layered sequences of the Panzhihua intrusion: a) and b) oxide-bearing lower zone, c) upper zone; d) syenitic dykes in the ultramafic rocks of the Hongge intrusion; e) layered gabbro and f) gabbroic pegmatite of the Baima intrusion.

volcanoclastics of the Xuanwei Formation, which is a continental facies in places. The variable thicknesses of the Maokou Formation were used to support the presence of a domal structure prior to the eruption of the flood basalts. The ELIP is divided into marginal and central parts according to the doming structure (Xu et al., 2004). The Panxi region in the central-western part of the ELIP is covered mostly by high-Ti flood basalts (Qi et al., 2008; Qi and Zhou, 2008). In other places, both high-Ti and low-Ti basalts are spatially associated (Song et al., 2006; Wang et al., 2006). There are also possible Permian flood basalts west of the Songpan-Ganze Terrane. These basalts have identical geochemical features to the Emeishan basalts and are taken as evidence of rifting after emplacement of the Emeishan mantle plume (Song et al., 2004).

Some mafic-ultramafic intrusions in the ELIP host magmatic sulfide deposits and others host magmatic oxide deposits (Zhou et al., 2008). Those hosting sulfide deposits include mafic-ultramafic sills in the Yangliuping area to the north (Song et al., 2003, 2006, 2008) and the Jinping-Songda area to the southeast

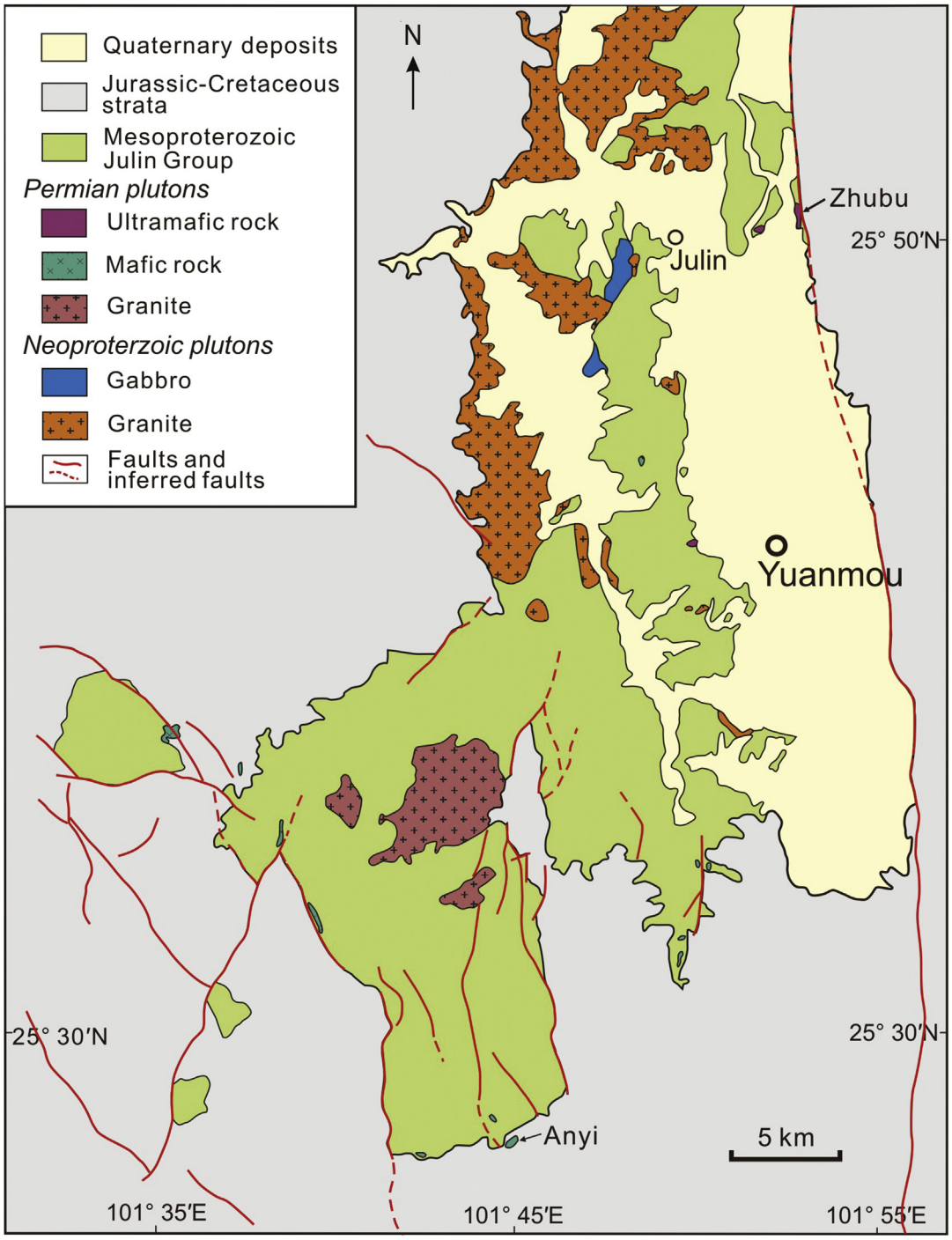

Figure 4. A simplified geological map of the Anyi-Yuanmou area, south of Panxi (modified after the Dayao 1:200,000 geological map of the Yunnan Geological Survey). Note that the Zhubu sulfide-bearing mafic-ultramafic intrusion to the north and that oxide-bearing Anyi intrusion to the south.

(Wang and Zhou, 2006; Wang et al., 2006) (Fig. 1). The Limahe sulfide deposit is in the Panzhihua area, central ELIP (Tao et al., 2010). The Jinbaoshan ultramafic sill in the Dali area hosts a Pt-Pd deposit (Wang et al., 2005, 2008a, 2010; Tao et al., 2007), and the Zhubu intrusion, south of Panzhihua, is also mineralized with Pt and Pd enrichment. Although these deposits are economic and are mined for Cu-Ni-(PGE) sulfides, they are generally small in size. Conversely, there are several world class Fe-Ti-(V) oxide deposits which are mainly distributed in the Panxi region along major N–S trending faults (Fig. 1). In the Funing area of the eastern part of the ELIP, both oxide and sulfide mineralization are present (Zhou et al., 2006; Wang et al., 2011).

3. Oxide-bearing mafic-ultramafic intrusions

3.1. Oxide-bearing mafic-ultramafic intrusions in the Panxi region

Oxide-bearing intrusions are mainly distributed in the Panxi region, the central ELIP, along major N–S-trending faults (Zhang et al., 1988; Zhou et al., 2005; Zhang et al., 2009) (Figs. 1 and 2). The oxide deposits in the Panxi region include those at Taihe, Xinjie, Baima, Hongge, and Panzhihua (Fig. 2). Among these, the Hongge deposit is the largest, followed by the Panzhihua and Baima deposits.

The Panzhihua intrusion is relatively well known (Zhou et al., 2005; Pang et al., 2008a, 2009; Hou et al., 2011, 2012, 2013). The intrusion is commonly interpreted to be a sill-like body, ~19 km long and ~2–3-km thick, which intrudes the Neoproterozoic Dengying limestones. Pecher et al. (2013), however, consider that the central portion is discordant. Contact metamorphism has produced a ~300 m wide contact aureole of marble and skarns in the rocks at the margin of the intrusion.

To the northwest, the intrusion is in fault contact with Triassic clastic sedimentary rocks and syenitic rocks (Ganino et al., 2008). From the base upward or from the margin inward, the intrusion is divided into marginal, lower, middle and upper zones (Zhou et al., 2005; Pang et al., 2008a, 2009; Pecher et al., 2013). The marginal zone consists of microgabbros and coarse-grained, isotropic and, in many places, pegmatitic gabbros. Both the middle and lower zones are dominated by layered gabbros. The upper zone is composed of layered gabbros with well-developed modal layering marked by alternating plagioclase- and clinopyroxene-rich layers (Fig. 3).

The Hongge intrusion is a NNE-striking elongated lopolith, approximately 16 km long and 3–6 km wide, with an exposed area of ~60 km^2 (Panxi Geological Team, 1987; Zhong et al., 2002). The intrusion dips east to northeast at a shallow angle and the exposed body varies in thickness from ~580 m to 2.7 km. The footwall of the intrusion is the middle Neoproterozoic Hekou Formation, composed of amphibolite and dolomitic limestone. The hanging wall is the Emeishan flood basalts, and in places the Sinian Dengying Formation, which is composed of dolomitic limestone. The intrusion and footwall rocks are crosscut by a series of NS-, NE- and NW-trending faults and folds. Numerous contemporaneous syenitic dykes make up ~ 29 vol.% of the intrusion, covering a surface area of 24 km^2 (Zhang et al., 1999). The Hongge intrusion is composed of a lower zone of olivine clinopyroxenite, middle zone of olivine clinopyroxenite, dunite, and anorthosite, and an upper zone of gabbro. Both the lower and middle zones also contain minor wehrlite and dunite.

Unlike the other intrusions in the Panxi region, the Baima intrusion is surrounded by granitic plutons that have zircon U-Pb ages of ca. 260 Ma and are therefore contemporaneous with the mafic members of the ELIP (Fig. 2) (Shellnutt and Zhou, 2007, 2008; Shellnutt et al., 2008, 2009a,b, 2010b). It is a 24-km long and 2–6.5-km wide sill-like body with an exposed surface area of ~100 km^2. It locally intrudes the ~1.0 Ga Huili Group which has been metamorphosed to marble and schist and the Sinian Dengying Formation of carbonate rocks (now marble) along the contact. Abundant syenitic dykes crosscut the intrusion. The intrusion is composed of a lower cumulate zone mainly of dunite, troctolite and olivine pyroxenite, a middle zone of olivine gabbro, and an upper zone of gabbro. Notably a 100–500 m wide, N–S trending gabbroic pegmatitic zone is present along the bottom of the lower zone, separating the mafic-ultramafic body from the syenites. The basal zone varies from 80 to 250 m in thickness. The middle olivine gabbro zone is 100–200 m thick, whereas the upper massive gabbroic zone is 1000–2000 m thick. The lower zone has well-developed mineralogical layering characterized by alternating dark and light bands. The oxides (40–55 vol.%) are associated with dunite and peridotite. These rocks consist of olivine and titanomagnetite-dominated cumulates with variable amounts of plagioclase, clinopyroxene, hornblende, ilmenite, spinel and sulfides as magmatic phases.

Most of the Hongge intrusion consists of ultramafic rocks in the middle and lower zones, whereas both the Panzhihua and Baima intrusions are mainly gabbroic with only minor ultramafic components. In addition to these three intrusions, the Xinjie intrusion contains both sulfide and oxide horizons, and exhibits mafic-ultramafic layering (Zhou et al., 2002a; Wang et al., 2008b).

All the intrusions in the Panxi region are typical layered intrusions. Most of the mafic and ultramafic rocks are rhythmically layered on a centimeter-scale, as in the Skaergaard intrusion (Wager and Brown, 1968; McBirney, 1996) and the Bushveld Complex (Eales and Cawthorn, 1996; Lee, 1996; Cawthorn and Spies, 2003). Individual bands can be traced laterally for several kilometers. The layering is mostly manifested in varying proportions of dark and light minerals with layers typically grading from a well-defined ultramafic base rich in clinopyroxene and olivine upward into leucogabbro or even anorthosite (Fig. 3).

3.2. Anyi intrusion

The Anyi intrusion is located in the Mouding-Yuanmou area, about 130 km south of Panzhihua (Figs. 1 and 4). In this region, the basement rocks are schist and marble of the ~1.0 Ga Julin Group distributed along N–S-trending faults west of Yuanmou (Fig. 4). The basement rocks are unconformably covered by Triassic–Jurassic sedimentary rocks of continental facies. Intruding the Julin Group are Neoproterozoic granite and middle Permian

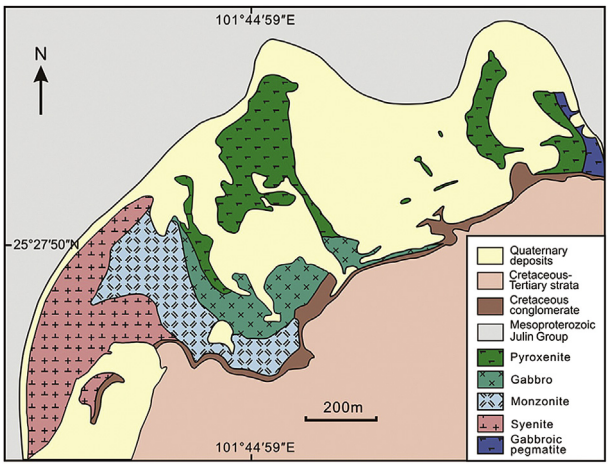

Figure 5. A simplified geological map of the Anyi intrusion (after local geological report).

granitic and mafic-ultramafic plutons including the ~260 Ma sulfide-bearing Zhubu intrusion (Fig. 4) (Zhou et al., 2002b).

The Anyi intrusion has a felsic portion comprising monzonite and syenite and a mafic-ultramafic portion of pyroxenite and gabbro (Fig. 5). It intrudes the Julin Group to the north and is unconformably overlain by Cretaceous conglomerate and mudstone to the south (Fig. 6a and b).

The monzonites are distributed in the southwest of the complex with an approximate thickness of 50–100 m. They have granular textures and are composed of equal amounts of plagioclase and K-feldspar with less than 25 vol.% pyroxene and hornblende (Fig. 6e). Syenites intrude the monzonite (Fig. 6c) and are composed of coarse-grained (~5 mm), reddish K-feldspar and biotite (Fig. 6d).

The mafic-ultramafic body is ~840-m long and ~300-m wide, exposed as an oval lopolith and dipping 50–20° to the center, and intruded by syenites (Fig. 5). Pyroxenite is transitional to gabbro with increasing plagioclase from the base upward. The lower zone of pyroxenite is composed dominantly of clinopyroxene with interstitial plagioclase, biotite and Fe-Ti oxides (Fig. 13a and b). Gabbro makes up the upper part of the body, which is 60–120 m thick. It is mainly composed of medium- to fine-grained clinopyroxene and plagioclase, with minor biotite, and shows typical layered structure.

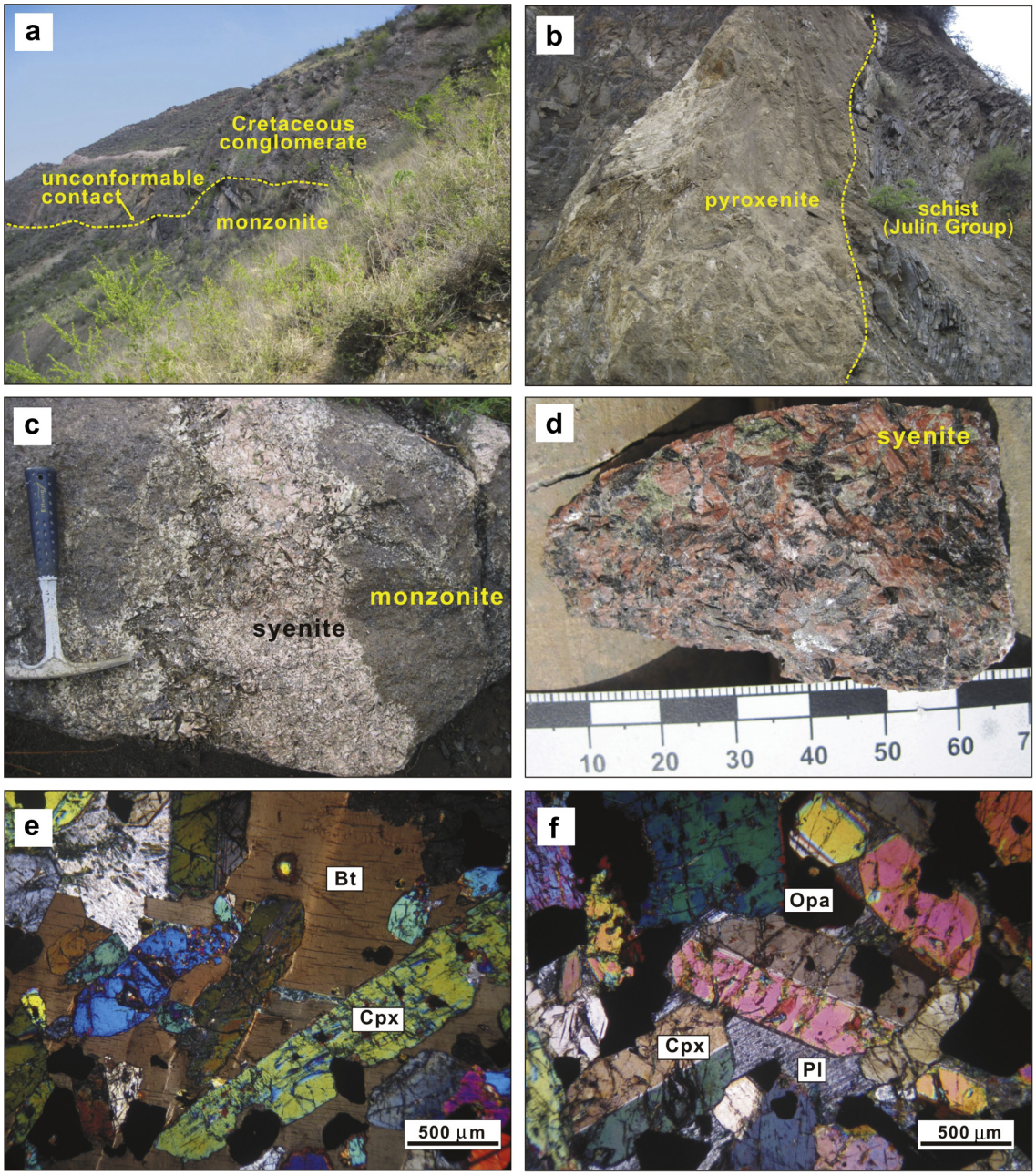

Figure 6. Field relationships of different rocks in the Anyi igneous complex. a) Cretaceous conglomerate is unconformably overlain by monzonite; b) intrusive contact of pyroxenite with the Julin Group; c) syenite intrudes monzonite; d) coarse-grained syenite; e) and f) pyroxenite is composed of clinopyroxene and interstitial biotite, plagioclase, opaque minerals. Abbreviations: Bt–biotite; Cpx–clinopyroxene; Pl–plagioclase; Opa–opaque minerals.

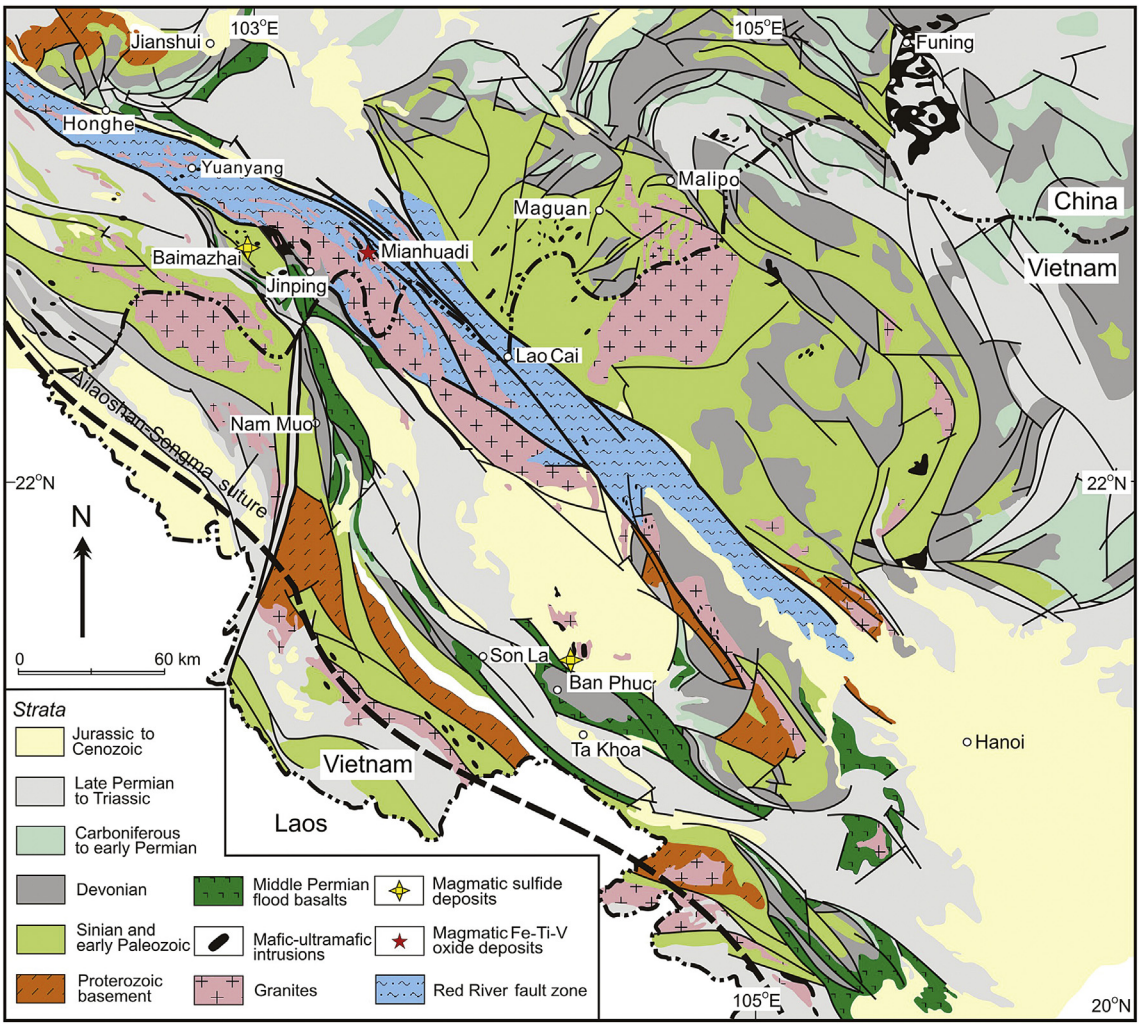

Figure 7. A simplified geological map showing the distribution of flood basalts and mafic-ultramafic intrusions in the Jinping-Songda area, Southern Yunnan and Northern Vietnam (after 1:1,000,000 Yunnan Geological Map and Vietnamese Geological Map, modified from Wang et al., 2007).

3.3. Mianhuadi intrusion

In the Jinping-Songda region of the southeastern part of the ELIP, both high-Ti and low-Ti basalts and picrites are present (Fig. 7) (Wang et al., 2007; Hanski et al., 2010). Associated with these volcanic rocks are mafic-ultramafic intrusions that intrude Devonian and Silurian sedimentary rocks. Some of these intrusions host magmatic Ni-Cu sulfide deposits, including the Baimazhai and Ban Phuc sulfide deposits (Fig. 7).

Several Permian mafic-ultramafic intrusions occur in the Red River fault zone, Yunnan Province, nearby Jinping (Figs. 7 and 8). The distribution of these intrusions may be related to displacement by the Red River fault zone (Chung and Jahn, 1995). In the Dapo-Mengqiao area, several small plutonic bodies are aligned NW–SE, roughly consistent with the foliation of the host rocks (Peng, 2009). They are hosted in the Ailaoshan Group, which is composed of schists, marble, amphibolites, gneisses and migmatite, and may represent dismembered bodies from one or more larger layered intrusions. These bodies are, in turn, intruded by early Mesozoic granitic plutons. Both the mafic-ultramafic rocks and granites have undergone extensive metamorphism up to amphibolite facies. Locally, these rocks show strong schistosity and are strongly foliated and/or tightly folded (Fig. 9b). However, primary gabbroic textures are locally preserved.

The oxide-bearing Mianhuadi mafic-ultramafic intrusion, the largest in the area, consists of amphibolite, plagioclase-bearing pyroxenite, olivine-amphibole pyroxenite, titano-augite pyroxenite and minor gabbro and anorthosite (Fig. 9a). Different phases of

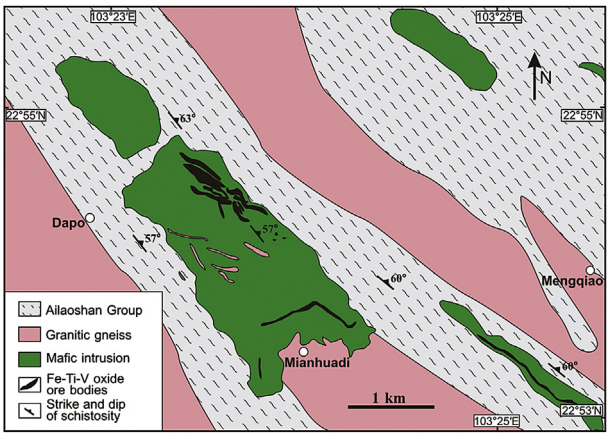

Figure 8. A simplified geological map of the Dapo-Mianhuadi-Mengqiao region in the Red River fault zone (after local geological map). Note that mafic-ultramafic intrusions and younger granitic plutons.

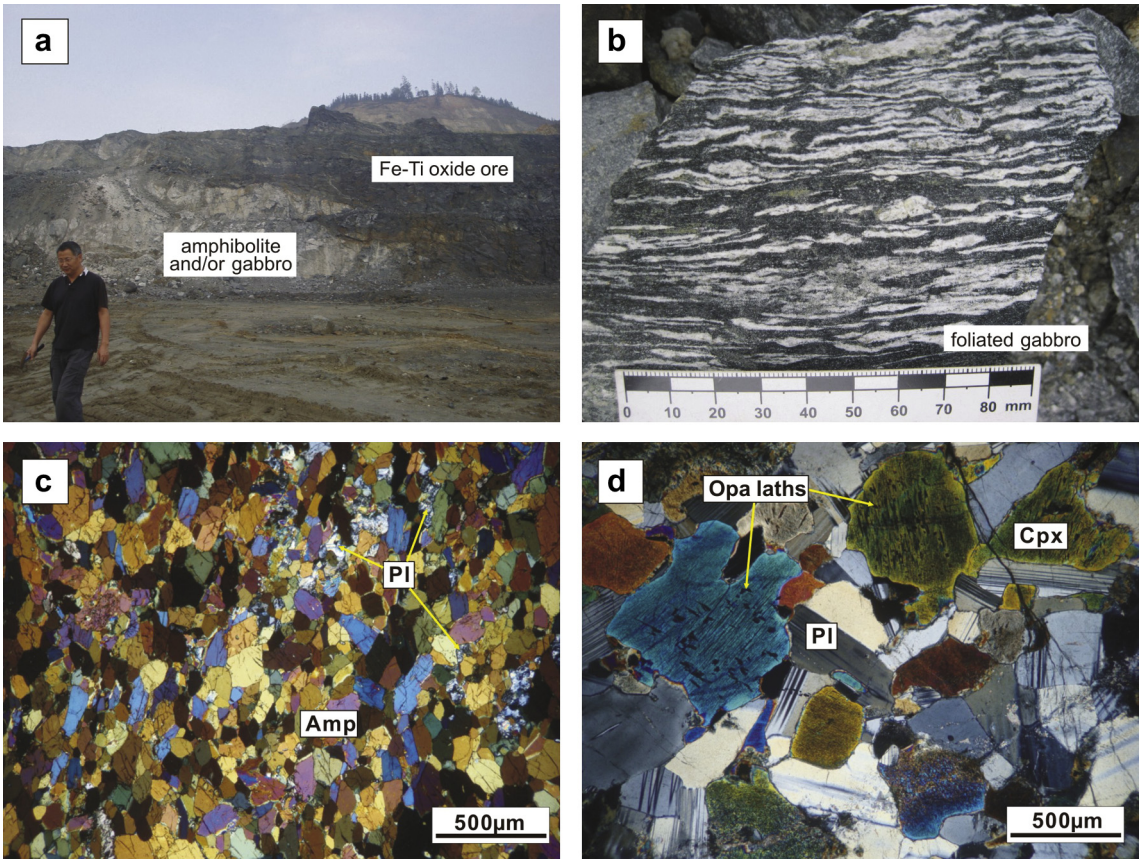

Figure 9. Field photos and photomicrographs of different rocks in the Mianhuadi intrusion. a) Irregular Fe-Ti oxide ore body is hosted in gabbro and amphibolite. Note that both ores and hosting rocks are extensively deformed; b) extensively foliated gabbro (amphibolite); c) amphibolite is composed dominantly of amphibole and plagioclase. Cross-plane; d) gabbro is composed of plagioclase and clinopyroxene with typical gabbroic texture. Cross-plane. Abbreviations: Pl–plagioclase, Amp–amphibole, Opa–opaque minerals, Cpx–clinopyroxene.

the Mianhuadi intrusion contain variable amounts of plagioclase (5–50 vol.%), clinopyroxene (15–80 vol.%), amphibole (30–80 vol.%) and subordinate olivine (0–10 vol.%), biotite (5–15 vol.%), Fe-Ti oxides (<15 vol.%) and minor sulfides (Fig. 9c and d). Fe-Ti oxides occur as interstitial fillings between the silicate minerals, or as euhedral and rounded grains enclosed in the silicate minerals (Fig. 9e).

4. Deposit geology and petrography of Fe-Ti oxide ores

4.1. Deposits in the Panxi region

Oxide ores of the deposits in the Panxi region mainly occur in the lower parts of the intrusions, and they generally form ore layers parallel to the layering of the intrusions (Fig. 10a and b). Oxide-rich and oxide-poor layers commonly alternate throughout the sequence. In the Panzhihua deposit, both the marginal and lower zones have the most extensive Fe-Ti oxide ores as massive to semi-massive bodies with thicknesses up to a few tens of meters. Layers and horizons with disseminated Fe-Ti oxides are also present in the middle zone but are much less extensive. Abundant net-textured ores occur mainly in the lower zone of the Hongge intrusion. In the Baima deposit, abundant net-textured or disseminated Fe-Ti oxide ores occur as layers or lenses in the basal cumulate zone. Net-textured ores are usually transitional to both massive and disseminated ores and are similar texturally to magmatic Ni-Cu sulfide ores.

Massive ores contain >85 vol.% Fe-Ti oxides (Fig. 10c); net-textured ores have 20 to 60 vol.% Fe-Ti oxides (Fig. 10d) and disseminated ores have <20 vol.% Fe-Ti oxides. These ores contain plagioclase, clinopyroxene and olivine as gangue minerals, and grains of these minerals are commonly surrounded by oxides; for example, net-textured ores have interconnected Fe-Ti oxide minerals, forming a groundmass that encloses cumulus silicate minerals such as olivine, clinopyroxene or plagioclase, or a combination of these minerals. Rims of hornblende surround both clinopyroxene and plagioclase, but not olivine (Fig. 11e–h). Clinopyroxene grains are Fe-Ti-rich, and contain two sets of exsolved lamellae marked by titanomagnetite and minor ilmenite laths parallel to prismatic cleavage planes.

In the oxide ores, the major ore minerals are titanomagnetite and ilmenite. Titanomagnetite occurs as polygonal crystals and typically accounts for ~85 vol.% of the opaque minerals. It contains exsolution lamellae including ilmenite and spinel (Fig. 12). Ilmenite occurs either as lamellae in titanomagnetite or as medium-grained irregular to polygonal crystals, and makes up another 15 vol.% of the ores (Fig. 12b–d). Subordinate Mg-Al spinel (<2 vol.%) is present as micro-patches distributed along the rims of ilmenite grains or as single irregular crystals at titanomagnetite and ilmenite grain boundaries (Fig. 12a and c). Minor sulfides (<1 vol.%) are sparsely disseminated both in the silicate minerals and the Fe-Ti oxides (Fig. 12d). There are also variable amounts of apatite.

4.2. Anyi deposit

This deposit contains mostly disseminated oxide ores hosted in pyroxenites and distinguished by minor but significant

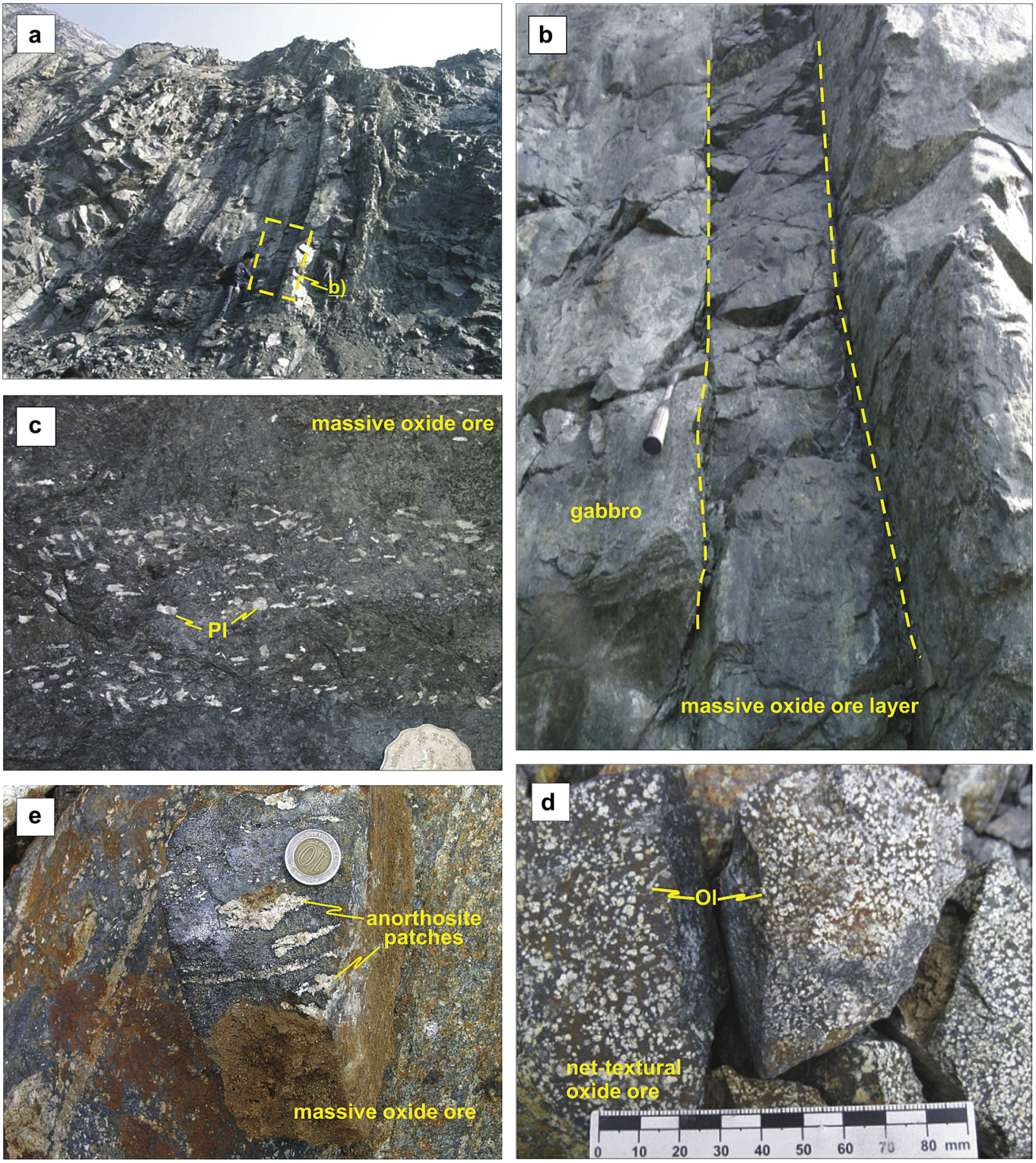

Figure 10. Field photos of different oxide ores in the Panxi region. a) and b) A massive magnetite layer in the Panzhihua intrusion; c) a massive oxide ore with plagioclase; d) a net-textured oxide ore with weathered olivine grains, Hongge mine; e) massive oxide ores with anorthosite patches, Hongge intrusion.

amounts of sulfides. They contain 0.2–0.5 ppm (Pt + Pd), but a low grade of FeO (15–17 wt.%) with an overall ore reserve of 66.7 Mt (local geological report). These disseminated ores are composed mainly of clinopyroxene (75 vol.%), and titanomagnetite and ilmenite (10–15 vol.%), and minor sulfide, plagioclase and biotite, with or without olivine (Fig. 13). Titanomagnetite and ilmenite occur as either polygonal crystals or interstitially between silicate minerals (Fig. 13a and b). Plagioclase is an interstitial phase set between cumulus clinopyroxene, and is usually albitized (Fig. 13c). Hornblende and biotite usually exhibit poikilitic texture, enveloping clinopyroxene and Fe-Ti oxide minerals (Fig. 13d).

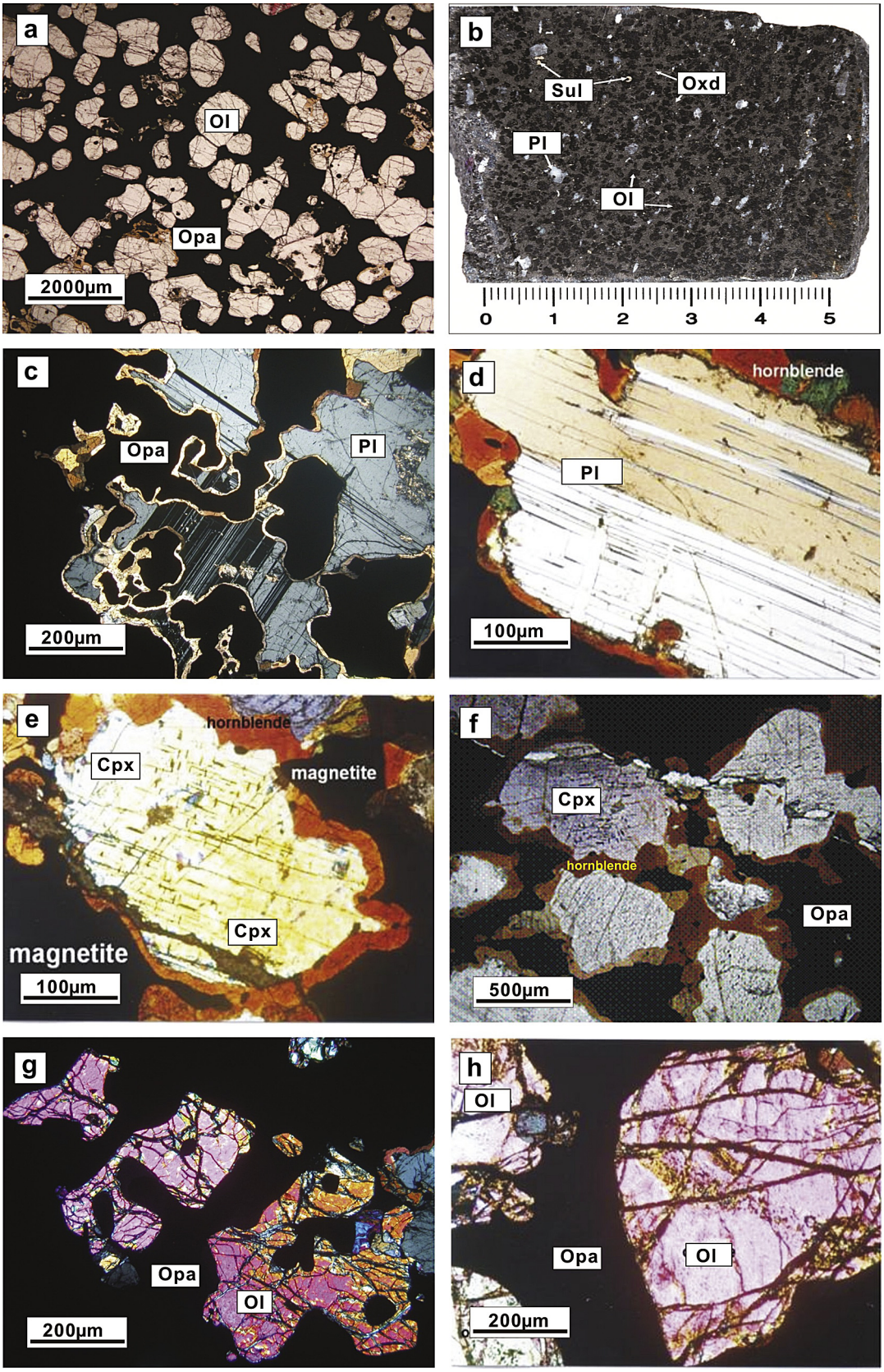

Figure 11. Photomicrographs of Fe-Ti oxide ores in the Panxi region. a) and b) Net-textured ore is composed of olivine grains which are surrounded by matrix of Fe-Ti oxides and minor sulfides; c) and d) plagioclase grains are eroded by matrix of Fe-Ti oxides, and there are hornblende rims between plagioclase and opaque minerals; e) and f) there are hornblende rims between clinopyroxene grains and Fe-Ti oxides; g) and h) olivine grains are surrounded or disturbed by matrix of Fe-Ti oxides. There are no hornblende rims between them. Photo c is adopted from Pang's PhD thesis (unpublished, 2008). Abbreviations: Ol–olivine, Sul–sulfides, Oxd–oxides, Pl–plagioclase, Opa–opaque minerals, Cpx–clinopyroxene.

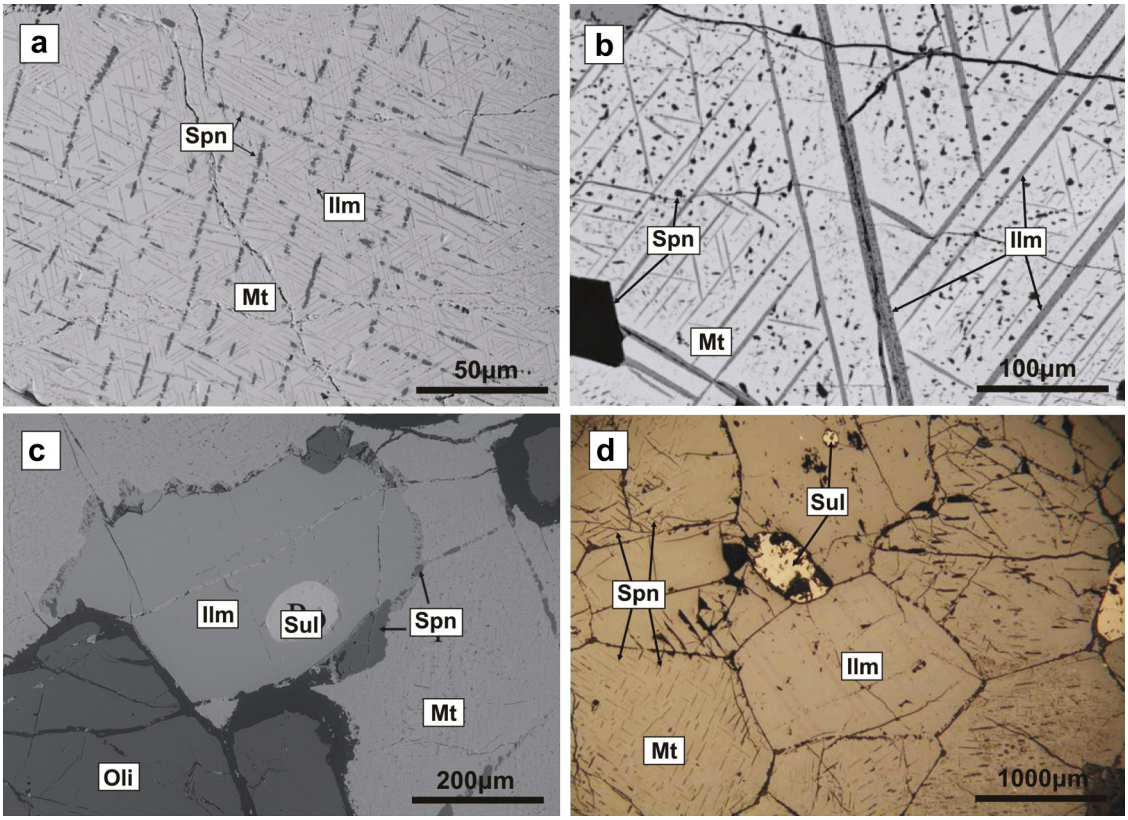

Figure 12. Subsolidus exsolution textures of titanomagnetite in the Panxi region. Photo d is taken from Pang et al. (2008a). Abbreviations: Spn-spinel, Ilm-ilmenite, Mt-titanomagnetite, Sul-sulfides, Oli-olivine.

4.3. Mianhuadi deposit

The deposit has recently been mined in an open pit and underground (Luo, 2007; Peng, 2009; Gai, 2010). More than 20 Fe-Ti oxide ore bodies occur as lenses and bands extending together with the host intrusion along a NW–SE direction.

The Dapo mine has 9 ore bodies that account for >50% of total reserves of this deposit. This mine alone has a total ore resource of 10.15 Mt with an average ore grade of 33.7 wt.% Fe, 9.69 wt.% Ti and 0.30 wt.% V (Gai, 2010). Fe-Ti oxide ores are principally hosted in amphibolites and olivine-amphibole pyroxenites (Fig. 9a). Fe-Ti oxide ores are mostly massive to semi-massive, and are commonly deformed or foliated (Fig. 9c and d). There are also subordinate disseminated and net-textured ores.

The Fe-Ti oxide ores contain small amounts of the same silicate minerals as the host rocks, but their concentrations and distribution are highly variable. Clinopyroxene in both the Fe-Ti oxide ores and the host silicate rocks generally shows two sets of exsolved lamellae marked by Fe-Ti oxide laths along prismatic cleavages (Fig. 14b). Fe-Ti oxides are dominated by titanomagnetite with subordinate ilmenite and spinel. Slightly deformed massive or semi-massive ores commonly display a granular texture consisting of medium to coarse polygonal grains of titanomagnetite and ilmenite whose boundaries are straight to slightly curved with distinct triple junctions with ~ 120° interfacial angles (Fig. 14e). In net-textured Fe-Ti oxide ores, silicate minerals occur as aggregates or isolated grains, surrounded or disrupted by aggregated titanomagnetite and ilmenite (Fig. 14d).

Titanomagnetite in the Mianhuadi deposit commonly exhibits complex subsolidus exsolution lamellae. These grains were generally recrystallized to larger polygonal grains, and commonly contain trellis and sandwich ilmenite lamellae (Fig. 14e). Subsolidus exsolution of titanomagnetite can also produce internal and external granules of ilmenite, but both kinds of ilmenite grains are free of exsolution (Fig. 14f). Patches and fine lamellae of aluminous spinel generally occur along the (110) plane in the inner parts of the host titanomagnetite (Fig. 14e and f). However, there are also external granules along grain boundaries between titanomagnetite and ilmenite. These textures are similar to those of oxide ores in the Panxi area, but it is not certain if these are purely igneous.

5. Ages of hosting intrusions

5.1. Mianhuadi intrusion

Zircon grains from the intrusion were analyzed for U-Pb isotopes using the Nu Instrument MC-ICPMS, attached to a Resonetics RESOlution M-50-HR Excimer Laser Ablation System, at the University of Hong Kong. Analyses were performed with a beam diameter of 30 μm, at a 6 Hz repetition rate. Data acquisition started with a 30 s measurement of gas blank during the laser warm-up time. The typical ablation time was 40 s for each measurement, resulting in pits of 30–40 μm depth. ^{232}Th, ^{208}Pb, ^{207}Pb, ^{206}Pb, ^{204}Pb were simultaneously measured in static-collection mode. External corrections were applied to all unknowns, and zircon standards 91500 and GJ were used as external standards and were analyzed twice before and after every 10 analyses.

Twenty-five zircon grains from a metagabbro sample (MS11-05) were analyzed. They have low to moderate U (57.8–192 ppm) and Th (20.1–106 ppm) with Th/U ratios mostly ranging from 0.5 to 1.5 (Table 1). More than half of the analyses are concordant (Fig. 15). These analyses with concordant ages yield a mean ^{206}Pb/^{238}U age of 259.6 ± 0.8 Ma (MSWD = 0.39; Fig. 15). Four younger grains (spots

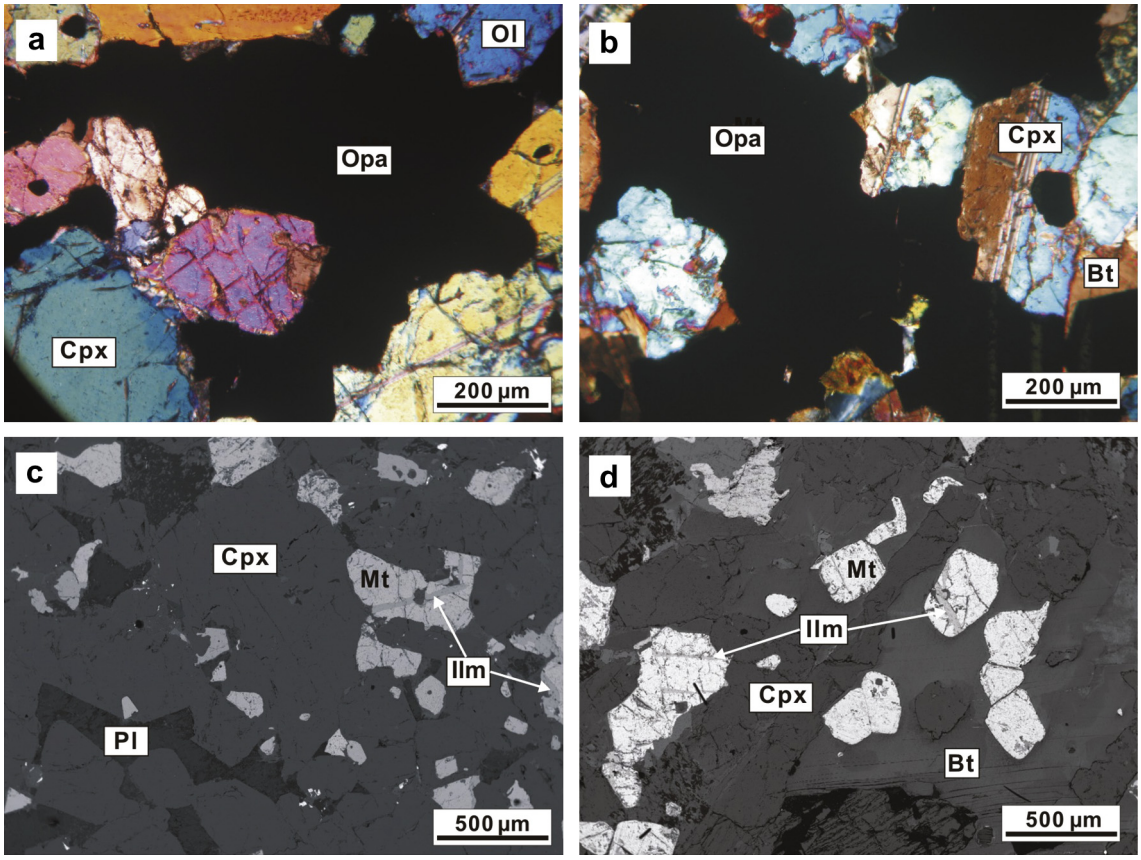

Figure 13. Photomicrographs of disseminated oxide ores of the Anyi deposit. a) and b) Titanomagnetite occurs as interstitial mineral between silicate minerals; c) and d) titanomagnetite occur as euhedral grains enclosed in biotite or as interstitial phases between silicate minerals. Note that some grains contain exsolution of ilmenite lamellae. Abbreviations: Opa–opaque minerals; Cpx–clinopyroxene; Bt–biotite; Ol–olivine; Pl–plagioclase; Mt–magnetite; Ilm–ilmenite.

08, 14, 23 and 25) may be metamorphic in origin, and have not been included in the age calculation.

5.2. Intrusions in the Panxi region

A large number of zircon U-Pb age dates for intrusions in the Panxi region have already been published in the past and are summarized in Fig. 16. The first age was published by Zhou et al. (2002a) for the Xinjie intrusion. Notably all these oxide-bearing intrusions and some of the associated syenitic plutons have an age of ca. 260 Ma (Zhong and Zhu, 2006; Zhong et al., 2007, 2009; Shellnutt and hou, 2008; Zhou et al., 2008; Shellnutt et al., 2009a, 2011, 2012). In the Panxi region, some other intrusions, notably Nantianwan, Jinbaoshan, Zhubu and Limahe, are also dated at ~260 Ma (Zhou et al., 2002a; Tao et al., 2009; Wang et al., 2012).

6. Chemical compositions of oxide minerals

Chemical compositions of oxide minerals from the Panxi region are available in the literature (Pang et al., 2008a, b; Wang et al., 2008b; Bai et al., 2012; Shellnutt and Pang, 2012). More than 700 analyses for both Cr-rich titanomagnetite and titanomagnetite from these references are listed in Appendix A. Ilmenite is abundant but not included, because exsolved grains from host titanomagnetite are abundant.

New major element analyses for oxide minerals from the Anyi and Mianhuadi deposits were determined with a JEOL JXA-8100 electron microprobe at the Guangzhou Institute of Geochemistry, Chinese Academy of Sciences, using a beam of 15 keV and 20 nA focused to a spot of ~2 μm in diameter. Peak and background counting times were set at 30 and 15 s, respectively. The standards used for oxide analyses were spinel for Mg and Al, diopside for Si, ilmenite for Ti, vanadium metal for V, chromite for Cr and Fe, manganese oxide for Mn, and niccolite (NiAs) for Ni. Because of overlap between Ti Kβ and V Kα peaks (Carmichael, 1967), V concentrations were corrected on the basis of analyses of V-free and Ti-bearing standards, rutile and native Ti. Concentrations of V after correction for the Ti Kβ peak are mostly less than 1 wt.%. Ferrous and ferric iron were estimated from stoichiometry and charge balance. The precision of the analyses is better than 5% for major elements.

6.1. Oxide minerals from the Panxi region

6.1.1. Cr-rich titanomagnetite

There is an unusual association of Cr-rich titanomagnetite and Cr-poor titanomagnetite in the Xinjie intrusion. Cr-poor titanomagnetite is interstitial between silicate minerals and may form Fe-Ti oxide-rich layers. Cr-rich titanomagnetite grains are usually euhedral to subhedral, and are enclosed within olivine or clinopyroxene of wehrlite and olivine pyroxenite of the lower part of the intrusion (Wang et al., 2008b). Some Cr-rich titanomagnetite grains contain $\leq$15% ilmenite exsolution lamellae, with the width of the lamellae generally $<$0.01 mm. They have high FeO^t ranging from 45 to 83 wt.%, and contain 6.6 to 29.9 wt.% Cr_2O_3, 0.49 to 8.8 wt.% Al_2O_3 and 0.09 to 2.9 wt.% MgO (Fig. 17). There are positive correlations between Cr_2O_3 and Al_2O_3 and negative correlations between Cr_2O_3 and Fe_2O_3. Al_2O_3 correlates positively with MgO (also see Fig. 9 of Wang et al., 2008b). Their TiO_2 contents vary widely from 1.2 to 22.8 wt.%, with the majority between 1.2 and 9.1 wt.%. This large

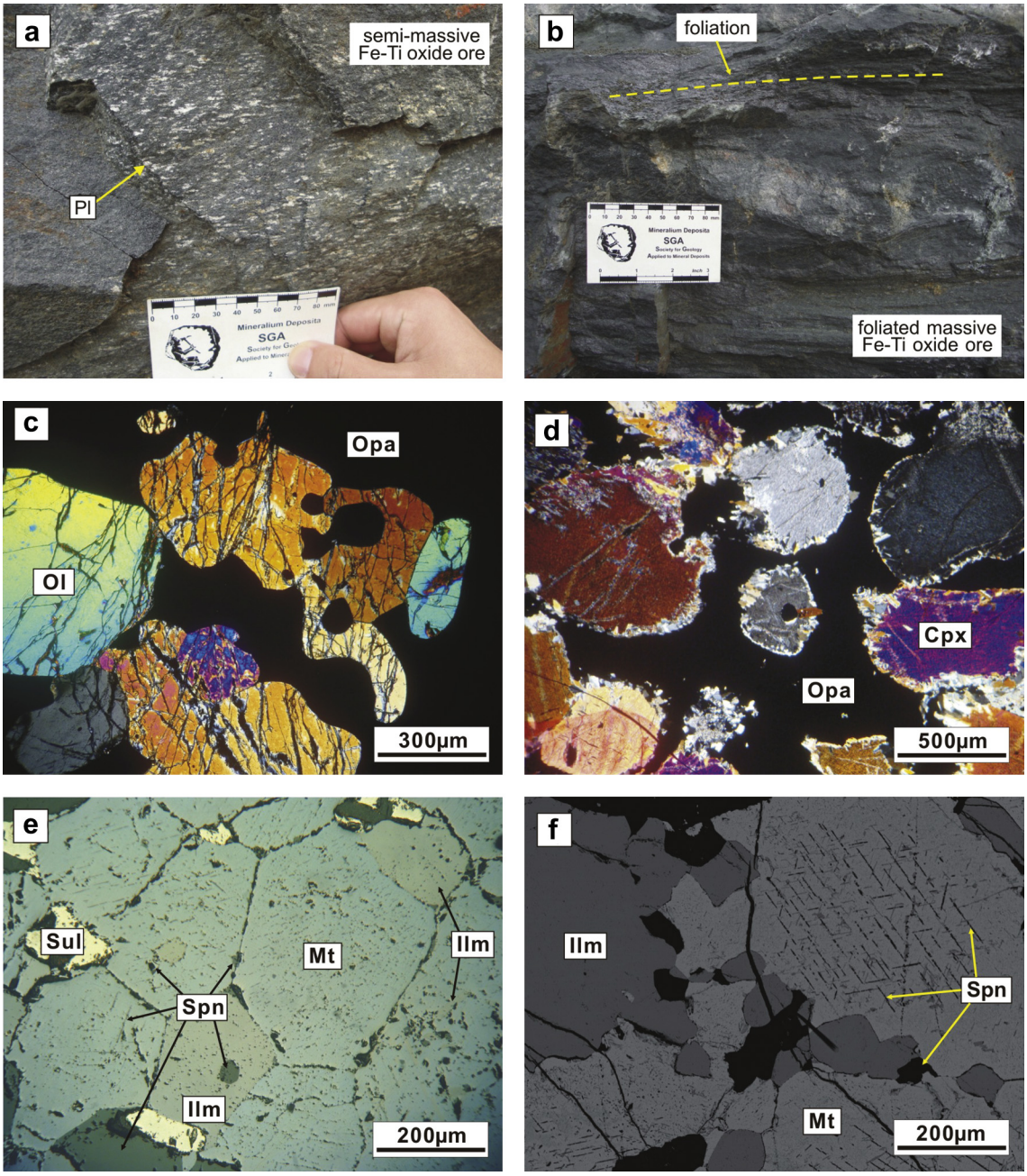

Figure 14. Field photos and photomicrographs of different ores in the Mianhuadi deposit. a) Semi-massive Fe-Ti oxide ores with plagioclase; b) foliated massive Fe-Ti oxide ore; c) Fe-Ti oxides occur as interstitial fillings among olivine or as grains enclosed by olivine. Cross-plane; d) net-textured oxide ore. Cross-plane; e) massive Fe-Ti oxide ore. Boundaries between titanomagnetite and ilmenite are straight to slightly curved and meet at distinct triple junctions with ~ 120° interfacial angles. There are also abundant exsolutions of ilmenite lamellae and spinel. Reflected light; f) subsolidus exsolutions textures of titanomagnetite. BSE image. Abbreviations: Pl—plagioclase; Amp—amphibole; Mt—titanomagnetite; Opa—opaque minerals; Cpx—clinopyroxene; Oli—olivine; Ilm—ilmenite; Spn—spinel; Sul—sulfides.

variation of TiO_2 may be potentially due to the variable exsolution of ilmenite (Wang et al., 2008b). Cr-rich titanomagnetite is also observed as inclusions in olivine and clinopyroxene in the ultramafic portions of both the Hongge and Baima intrusions (Wang and Zhou, 2013).

6.1.2. Cr-poor titanomagnetite

Titanomagnetite from different types of ores from the Panzhihua, Hongge and Baima deposits contains highly variable Ti with TiO_2 contents ranging from <0.1 to 30 wt.% (Fig. 17). This large variation is partially due to the exsolution of ilmenite. Titanomagnetite usually has significant amounts of Al_2O_3 (0.1–6 wt.%) and MgO (<0.1 to 4 wt.%) (Fig. 17). The compositional ranges of these elements for titanomagnetite from different deposits are slightly different (Fig. 17).

Titanomagnetite contains small amounts of Cr_2O_3, much lower than Cr-rich titanomagnetite (Fig. 17). Compositions of titanomagnetite show positive correlations of Al_2O_3, MnO, MgO and FeO with TiO_2 (Fig. 17).

6.2. Anyi deposit

Titanomagnetite in the Anyi ultramafic intrusion contains 7 to 24 wt.% TiO_2. It has variable amounts of minor elements, including

Table 1
LA-ICP-MS zircon U-Pb analyses for a metagabbro from the Mianhuadi intrusion.

Spot	Th	U	Th/U	$^{207}Pb/^{206}Pb$		$^{207}Pb/^{235}U$		$^{206}Pb/^{238}U$		$^{207}Pb/^{206}Pb$		$^{207}Pb/^{235}U$		$^{206}Pb/^{238}U$	
	ppm	ppm		Ratio	1σ	Ratio	1σ	Ratio	1σ	Age	1σ	Age	1σ	Age	1σ
MS11-05: Metagabbro															
01	61.9	121	0.51	0.0521	0.0001	0.2938	0.0019	0.0409	0.0003	300.1	3.7	261.5	1.5	258.3	1.7
02	20.1	174	0.12	0.0528	0.0001	0.2955	0.0018	0.0406	0.0002	320.4	3.7	262.9	1.4	256.4	1.4
03	68.6	105	0.66	0.0521	0.0003	0.2935	0.0017	0.0409	0.0002	287.1	13	261.3	1.3	258.4	0.9
04	106	57.8	1.83	0.0515	0.0002	0.2929	0.0019	0.0412	0.0002	264.9	7.4	260.8	1.5	260.4	1.5
05	97.8	79.1	1.24	0.0548	0.0008	0.2988	0.0046	0.0395	0.0002	405.6	31	265.5	3.6	249.8	1.2
06	43.3	153	0.28	0.0517	0.0001	0.2929	0.0017	0.0411	0.0002	333.4	5.6	260.8	1.4	259.6	1.3
07	82.6	88.5	0.93	0.0533	0.0002	0.2974	0.0021	0.0404	0.0002	342.7	11	264.4	1.6	255.5	1.2
08	52.6	148	0.36	0.0516	0.0001	0.2519	0.0016	0.0354	0.0002	333.4	3.7	228.1	1.3	224.2	1.4
09	71.2	110	0.65	0.0528	0.0003	0.2937	0.0027	0.0403	0.0002	320.4	13	261.5	2.1	254.9	1.3
10	91.7	68.3	1.34	0.0531	0.0001	0.2957	0.0024	0.0404	0.0003	331.5	8.3	263.0	1.9	255.1	1.7
11	95.8	77.4	1.24	0.0530	0.0005	0.2935	0.0032	0.0402	0.0001	327.8	22	261.3	2.5	254.0	0.8
12	66.9	114	0.58	0.0512	0.0001	0.2920	0.0020	0.0414	0.0003	250.1	7.4	260.1	1.6	261.2	1.7
13	50.3	145	0.35	0.0530	0.0003	0.2964	0.0038	0.0404	0.0004	331.5	13	263.6	3.0	255.3	2.2
14	82.9	100	0.83	0.0514	0.0001	0.2656	0.0020	0.0375	0.0003	257.5	7.4	239.2	1.6	237.3	1.7
15	59.6	112	0.53	0.0517	0.0007	0.2926	0.0037	0.0410	0.0002	272.3	29	260.6	2.9	259.3	1.5
16	93.0	84.0	1.11	0.0518	0.0001	0.2935	0.0016	0.0411	0.0002	279.7	5.6	261.3	1.3	259.5	1.5
17	75.2	102	0.74	0.0545	0.0001	0.3008	0.0015	0.0401	0.0002	390.8	7.4	267.0	1.1	253.2	1.2
18	83.7	98.7	0.85	0.0515	0.0001	0.2930	0.0018	0.0412	0.0002	264.9	38	260.9	1.4	260.5	1.5
19	71.5	118	0.61	0.0515	0.0001	0.2922	0.0019	0.0411	0.0003	264.9	36	260.3	1.5	259.8	1.7
20	100	72.3	1.39	0.0515	0.0001	0.2918	0.0017	0.0411	0.0002	261.2	38	260.0	1.3	259.6	1.4
21	68.2	116	0.59	0.0516	0.0001	0.2929	0.0028	0.0411	0.0004	333.4	7.4	260.8	2.2	259.7	2.2
22	65.3	121	0.54	0.0516	0.0001	0.2933	0.0018	0.0412	0.0002	264.9	5.6	261.1	1.4	260.5	1.5
23	22.1	192	0.12	0.0524	0.0001	0.2500	0.0013	0.0346	0.0002	301.9	5.6	226.6	1.0	219.1	1.0
24	31.4	142	0.22	0.0615	0.0003	0.3404	0.0049	0.0400	0.0005	657.4	4.6	297.5	3.7	253.1	2.8
25	62.9	123	0.51	0.0517	0.0002	0.2658	0.0018	0.0372	0.0002	276.0	9.3	239.3	1.5	235.7	1.2

No common lead is corrected.

0.1 to 4 wt.% Al_2O_3, <0.3 wt.% V_2O_3, <0.1 wt.% Cr_2O_3, 0.1 to 1.0 wt.% MnO and 0.1 to 3.0 wt.% MgO (Table 2). There are good positive correlations of FeO (35–55 wt.%), Al_2O_3 and MnO with TiO_2 (Fig. 17). Compared with other Fe-Ti-V oxide deposits in the Panxi region, the Anyi deposit has titanomagnetite compositions with lower MgO, V_2O_3 and Cr_2O_3 but higher TiO_2.

6.3. Mianhuadi deposit

Titanomagnetite in the Mianhuadi intrusion ranges from near end-member Fe_3O_4 to titanomagnetite containing up to 5 wt.% TiO_2 (Table 2). It has variable amounts of Al_2O_3 (0.35–2.45 wt.%), V_2O_3 (0.2–0.6 wt.%), Cr_2O_3 (0.1–0.8 wt.%), MnO (0.01–0.3 wt.%) and MgO

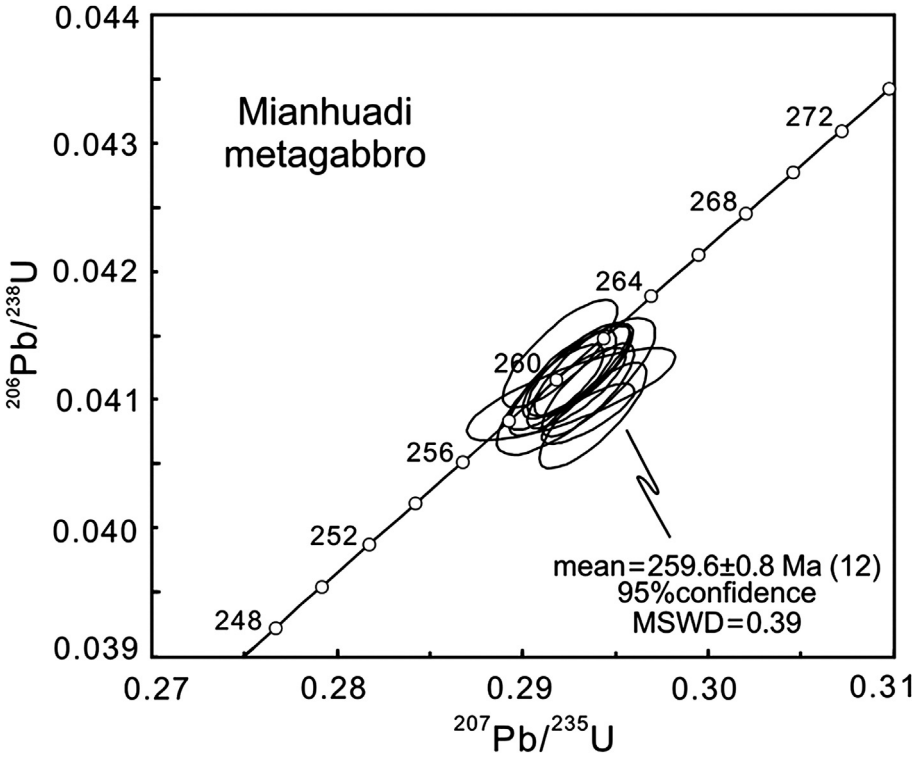

Figure 15. Concordia plots of U-Pb isotopic compositions for zircon grains from a metagabbro of the Mianhuadi intrusion.

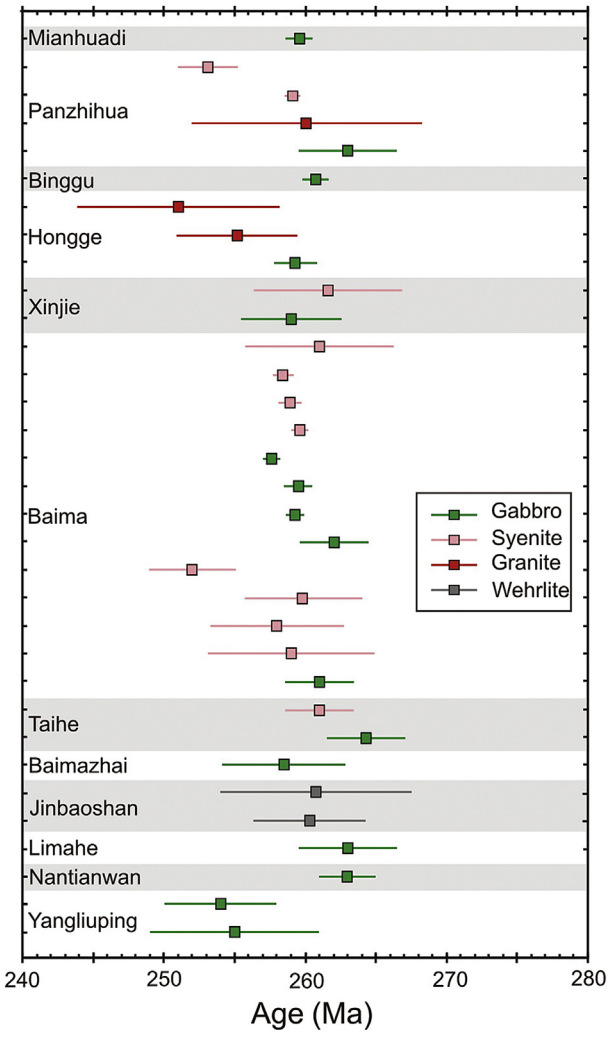

Figure 16. Compilation of available zircon U-Pb ages for ELIP mafic-ultramafic intrusions that contain either sulfide or oxide deposits. Note that the ages of spatially associated syenitic plutons with oxide-bearing intrusions are also included. Data sources: Zhou et al. (2002a, 2005, 2008); Song (2004); Zhong and Zhu (2006); Zhong et al. (2007, 2009); Shellnutt and Zhou (2008); Xu et al. (2008); Shellnutt et al. (2009b, 2011, 2012); Tao et al. (2009); Wang et al. (2012).

(0.1–0.7 wt.%). Compositions of titanomagnetite show positive correlations of Al_2O_3, MnO, MgO and FeO with TiO_2 (Fig. 17), similar to those of the oxide deposits in the Panxi region, suggesting the metamorphism did not strongly modify chemical compositions of titanomagnetite.

7. Discussion

7.1. Panzhihua-type deposits as a new type of magmatic Fe-Ti-V oxide deposit

Layered mafic-ultramafic intrusions usually contain layers of Fe-Ti-V oxide ores at relatively high levels in the intrusion, such as in the Bushveld Complex in South Africa and the Stillwater Complex in Montana (USA) (Bateman, 1951; Reynolds, 1985; Cawthorn, 1996). Major Fe-Ti-V oxide deposits are also hosted by anorthositic massifs (Bateman, 1951; Philpotts, 1967; Kolker, 1982). Together with heavy mineral deposits in beach sands, these deposits provide the major sources of Ti and V for the world. The Fe-Ti-V oxide ores in the ELIP deposits occur as massive, conformable lenses or layers in the lower parts of the host intrusion, rather than as stratiform "reef-style" magnetite layers higher in the intrusion, as is the case in the Bushveld and Stillwater complexes (Zhou et al., 2005; Pang et al., 2008a,b, 2009). Another unique feature of the deposits in the ELIP is the association of the titanomagnetite ores with either olivine, plagioclase or clinopyroxene, or a combination of these minerals. The major oxide minerals, titanomagnetite and ilmenite, may co-exist with early-formed Cr-rich titanomagnetite. Similar deposits are currently unknown elsewhere in the world, and we thus propose the term "Panzhihua-type" for the deposits in the ELIP.

7.2. Origin of the Panzhihua-type Fe-Ti-V oxide deposits

7.2.1. Crystallization of early Cr-rich titanomagnetite and late titanomagnetite

The Xinjie intrusion is a mafic-ultramafic layered intrusion that contains considerable amounts of ultramafic rocks, including wehrlite and olivine clinopyroxenite (Wang et al., 2008b). Abundant inclusions of Cr-rich titanomagnetite (Fe-rich chromite in Wang et al., 2008b) occur in olivine of the ultramafic rocks. Similar occurrences of this mineral are also found in the Panzhihua, Hongge and Baima intrusions (Pang et al., 2008b), but fewer analyses are available. The Cr-rich composition indicates that Cr-Fe-Ti oxides were on the liquidus early in the crystallization of the host magmas. Cr-rich titanomagnetite also occurs in the lower part of the layered sequences and may have crystallized contemporaneously with, or earlier than, olivine and clinopyroxene. This mineral has considerable amounts of TiO_2 (Fig. 17) and some grains have clear exsolution lamellae of ilmenite (Wang et al., 2008b).

Chromium has a high partition coefficient in Fe-Ti oxides, like magnetite ($D_{Cr}^{magnetite/melt} = 350$) (e.g., Duchesne, 1999). In early stages of mafic magma evolution, chromium is available and any oxide mineral that crystallizes must have considerable amounts of Cr. Cr-rich titanomagnetite of the Xinjie and other intrusions in Panxi may have formed in a manner similar to the early-formed chromite of ultramafic rocks from layered intrusions (Irvine, 1977). Although we do not know of any analog of such Cr-rich titanomagnetite elsewhere, the early crystallization of Cr-rich titanomagnetite rather than chromite may indicate a unique parental magma for these intrusions.

Pang et al. (2008a,b, 2009, 2010) explained the massive accumulation of titanomagnetite ores as a product of early crystallization. Bai et al. (2012) further proposed that the ore bodies formed in a magma flow-through (i.e., conduit) system like that envisaged for magmatic sulfide deposits. The low Cr content of the titanomagnetite ores (Fig. 17) makes it unlikely that they are the product of early crystallization from a basaltic magma. In addition, the interstitial nature of Cr-poor titanomagnetite of net-textured ores (Fig. 5) provides strong evidence for its crystallization later in the crystallization sequence (but see Duchesne (1999) who attributed this texture to subsolidus grain boundary readjustment). Of particular interest are obvious embayments in olivine, plagioclase and clinopyroxene which suggest that these silicate crystals are corroded by oxide minerals (Fig. 11). We believe that the best explanation is that Cr-poor titanomagnetite crystallized much later than these silicate minerals.

7.2.2. Evidence for and compositions of Fe-Ti-(P) rich oxide melts

Pang et al. (2008a) presumed that all Cr-poor titanomagnetite, ilmenite and hercynite in the massive ores at the basal part of the Panzhihua intrusion formed by subsolidus exsolution from a primary oxide, and calculated its composition as an aluminous titanomagnetite which is compositionally similar to the bulk composition of the most massive oxide ores. They considered that

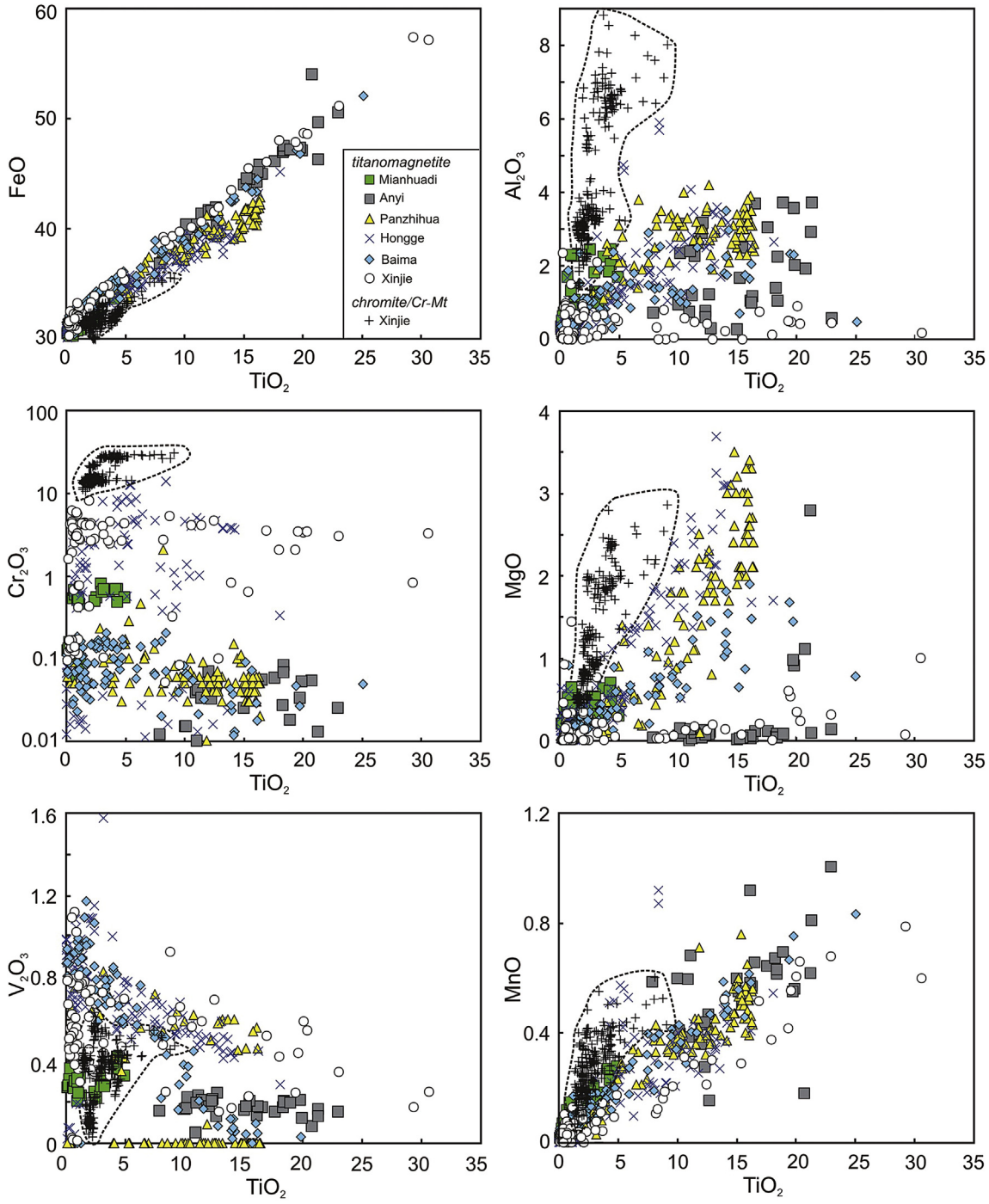

Figure 17. Bi-elemental variation diagrams (in wt.%) of titanomagnetite from the Mianhuadi and Anyi deposits. Also plots are compositions of titanomagnetite from the Panzhihua (Pang et al., 2008a), Hongge (Bai et al., 2012), Baima (Shellnutt and Pang, 2012), Xinjie (Wang et al., 2008b) deposits and composition of Cr-rich titanomagnetite from the Xinjie deposit (Wang et al., 2008b).

these ores formed from early accumulation of such an oxide mineral (Pang et al., 2008a). However, the textural relationships of oxide ores do not support the accumulation of a single oxide phase. The matrix of net-textured oxide ores is composed of several phases, including titanomagnetite, ilmenite, sulfide, apatite and hornblende, and encloses silicate minerals. Both ilmenite and hercynite can be products of subsolidus exsolution upon cooling, as described in Pang et al. (2008a) and elsewhere. It is possible that some large granular ilmenite grains may not represent exsolution products but have crystallized directly from melts (Fig. 12d). Apatite is abundant in some oxide ores in the Panzhihua intrusion (Zhou et al., 2005; Wang and Zhou, 2013), although absent from other ores, as indicated by P_2O_5 contents close to detection limits.

Based on textural relationships, Wang and Zhou (2013) proposed that large amounts of Cr-poor titanomagnetite (+ilmenite) and other minor phases have crystallized from Fe-Ti-(P) oxide melts to form net-textured and massive ores. Such melts should have minor amounts of Cr and V that were later incorporated into

Table 2
Representative analyses of titanomagnetite from the Mianhuadi and Anyi Fe-Ti-V oxide deposits.

Deposit	Mianhuadi									Anyi								
Sample	DP11-1			DP11-16			DP11-22			AY11-26			AY11-37			AY11-40		
Rock	Net-textured ore			Semi-Massive ore			Massive oxide ore			Disseminated ore								
SiO_2	0.04	0.13	0.08	0.12	0.05	0.16	0.06	0.05	0.05	0.04	0.03	0.02	0.04	0.03	0.17	0.11	0.05	0.12
TiO_2	0.41	1.31	0.20	1.18	0.69	0.97	2.62	2.40	4.97	7.92	10.95	16.13	12.05	21.24	10.18	12.06	19.75	11.03
Al_2O_3	0.74	1.07	0.51	2.29	1.71	2.30	2.44	1.07	1.71	0.74	0.74	1.05	2.89	2.93	3.16	3.17	3.58	2.41
Fe_2O_3	65.77	63.32	66.69	62.36	64.59	62.81	60.08	60.96	57.29	50.60	46.24	35.02	41.67	26.26	44.44	39.97	25.57	43.21
FeO	30.37	30.95	30.73	31.38	30.99	31.01	32.76	32.07	35.55	37.05	40.54	44.63	41.69	46.31	40.37	41.87	47.40	40.76
MnO	0.07	0.12	0.03	0.04	0.04	0.15	0.17	0.16	0.28	0.59	0.60	0.92	0.43	0.62	0.41	0.36	0.55	0.38
MgO	0.41	0.55	0.20	0.48	0.52	0.65	0.52	0.38	0.30	0.03	0.00	0.03	0.12	2.80	0.14	0.04	0.97	0.13
NiO	0.00	0.00	0.00	0.11	0.11	0.09	0.12	0.05	0.09	0.03	0.02	0.02	0.01	0.00	0.00	0.00	0.10	0.00
Cr_2O_3	0.11	0.07	0.13	0.45	0.67	0.54	0.55	0.49	0.54	0.01	0.04	0.00	0.07	0.01	0.02	0.07	0.03	0.01
V_2O_3	0.36	0.23	0.28	0.23	0.27	0.31	0.22	0.25	0.33	0.16	0.05	0.14	0.18	0.17	0.17	0.18	0.21	0.20
total	98.27	97.75	98.83	98.64	99.62	98.99	99.53	97.87	101.09	97.16	99.21	97.94	99.15	100.36	99.06	97.82	98.22	98.25
Based on 4 oxygen																		
Si	0.00	0.01	0.00	0.00	0.00	0.01	0.00	0.00	0.00	0.00	0.00	0.00	0.00	0.00	0.01	0.00	0.00	0.00
Ti	0.01	0.04	0.01	0.03	0.02	0.03	0.07	0.07	0.14	0.23	0.32	0.47	0.34	0.58	0.29	0.35	0.56	0.32
Al	0.03	0.05	0.02	0.10	0.08	0.10	0.11	0.05	0.08	0.03	0.03	0.05	0.13	0.12	0.14	0.14	0.16	0.11
Fe^{3+}	1.92	1.85	1.95	1.80	1.85	1.80	1.71	1.78	1.62	1.49	1.33	1.01	1.31	1.40	1.26	1.15	1.48	1.24
Fe^{2+}	0.99	1.01	1.00	1.01	0.99	0.99	1.04	1.04	1.11	1.21	1.30	1.44	1.18	0.72	1.27	1.34	0.72	1.30
Mn	0.00	0.00	0.00	0.00	0.00	0.00	0.01	0.01	0.01	0.02	0.02	0.03	0.01	0.02	0.01	0.01	0.02	0.01
Mg	0.02	0.03	0.01	0.03	0.03	0.04	0.03	0.02	0.02	0.00	0.00	0.00	0.01	0.15	0.01	0.00	0.05	0.01
Ni	0.00	0.00	0.00	0.00	0.00	0.00	0.00	0.00	0.00	0.00	0.00	0.00	0.00	0.00	0.00	0.00	0.00	0.00
Cr	0.00	0.00	0.00	0.01	0.02	0.02	0.02	0.02	0.02	0.00	0.00	0.00	0.00	0.00	0.00	0.00	0.00	0.00
V	0.01	0.01	0.01	0.01	0.01	0.01	0.01	0.01	0.01	0.00	0.00	0.00	0.01	0.00	0.01	0.01	0.01	0.01
Total	3.00	3.00	3.00	3.00	3.00	3.00	3.00	3.00	3.00	3.00	3.00	3.00	3.00	3.00	3.00	3.00	3.00	3.00

titanomagnetite or ilmenite. The coexistence of Cr-poor titanomagnetite, apatite, ilmenite, hercynite and amphibole and minor disseminated sulfides in oxide ores strongly supports the idea that the melts from which oxide ores formed may have had small but significant amounts of SiO_2, MgO, Al_2O_3, Cr_2O_3, H_2O, P_2O_5 and S.

A recent study of volatiles in minerals by Xing et al. (2012) using a step-heating mass spectrometer suggests the presence of CO_2 and H_2O in titanomagnetite from Hongge (e.g., 0.61%), at levels much higher than those of other minerals (e.g., 0.05%). Their work indicates that titanomagnetite, clinopyroxene and apatite in net-textured ores of the Middle and Upper zones of the Hongge intrusion contain abundant volatiles including H_2O, SO_2, CO_2 and H_2, mostly released at the middle and high temperature intervals between 1200 and 400 °C temperature intervals. The release of volatiles at high temperatures indicates that they were originally dissolved in crystal structures or trapped as fluid inclusions in the minerals (c.f., Zhang et al., 2007).

Xing et al. (2012) noted that Cr-poor titanomagnetite releases much more H_2O and CO_2 than clinopyroxene and apatite, especially at the 800–400 °C temperature interval. Water and CO_2 are generally considered to be incompatible during magma evolution so that they tend to be trapped in late crystallizing minerals (e.g., Zhang et al., 2009; and references therein). Therefore, relatively high volatile contents of Cr-poor titanomagnetite indicate that the Cr-poor titanomagnetite formed under more volatile-rich conditions, late in the crystallization sequence, further suggesting the presence of volatiles in the Fe-Ti-(P) oxide melts.

The oxide melts would be dense and cannot be transported for long distances. We consider that these Fe-Ti-(P) rich melts were immiscible with, and segregated from the gabbroic magmas (Zhou et al., 2005). Although massive and net-textured oxide ores solidified later than silicate minerals, they may have formed from Fe-Ti-rich liquids that probably co-existed with silicate minerals or formed early enough to be concentrated as massive, either concordant or discordant, oxide ore bodies. Because they were denser than the silicate magmas, they would have settled downward as sills and dikes, crosscutting early-formed silicate cumulates (e.g., Ripley et al., 1998). Fe-Ti-(P) rich melts may also incorporate plagioclase, olivine or clinopyroxene, forming net-textural ores, in a manner similar to that for the formation of net-textural sulfide ores. Unlike magmatic sulfide deposits, there are abundant disseminated oxide ores higher in the cumulate sequences of the oxide-bearing intrusions in Panxi. The silicate magmas themselves may also evolve to become saturated in Fe-Ti, leading to normal crystallization of magnetite at a late stage after the appearance of plagioclase. Disseminated magnetite that crystallized from the evolved silicate magmas has much lower Al_2O_3, MgO and Cr_2O_3 than that from Fe-Ti-rich melts.

Why an immiscible oxide melt occurs in silicate magmas is not known. Experimental results suggest that the addition of H_2O to calc-alkaline basaltic systems in subduction zones lowers the crystallization temperature of silicate minerals but has relatively little effect on magnetite liquidus temperatures (Sisson and Grove, 1993). Thus, Pang et al. (2008b) in their study of Panzhihua argued that the addition of H_2O would cause Fe-Ti oxides to appear early in the magma relative to other silicate phases because of the high crystallization temperature of the oxides. However, as previously suggested, more abundant volatiles in the Cr-poor titanomagnetite than silicate minerals at Hongge do not support early fractionation of these oxides. Howarth et al. (2013) have proposed that magma hydration occurred after the commencement of accumulation of the crystal pile, causing later precipitation and emplacement of the magnetite ore layer(s) as discordant units. Both CO_2 and H_2O in the magmas may have acted as fluxing agents to facilitate the appearance of immiscible oxide liquids in extremely Fe-Ti-rich gabbroic magmas (Reynolds, 1985). Water and CO_2-rich fluids may have also been introduced to the magmas through magma-wall rock interaction during or after the emplacement of the high-Fe gabbroic magmas (Ganino et al., 2008).

7.3. An integrated genetic model

7.3.1. Oxide-bearing intrusions formed from evolved magmas

It is possible that Fe-enrichment is a feature of the parental magma attributable either to the mantle source composition or conditions of partial melting. Oxide-bearing intrusions in the ELIP

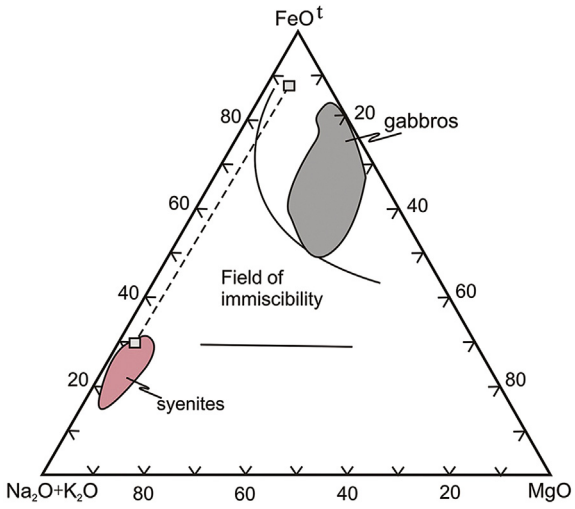

Figure 18. Triangle diagram showing magma evolution related to fluid immiscibility (after Philpotts, 1976, 1982). Also plotted are the composition of syenites and gabbros in the ELIP.

are thought to be related to the high-Ti series of rocks derived from the Emeishan mantle plume (Zhou et al., 2008). The primitive magmas for the high-Ti series may have had been Fe-picrites like those reported in Lijiang, western Yunnan (Zhang et al., 2006, 2008). These picrites contain olivine with relatively high Fo values (up to 89) (Hanski et al., 2010) and may represent the most primitive magma of the high-Ti series. The widespread high-Ti basalts may have formed by fractionation of Fe-picritic magmas.

Olivine from ultramafic rocks of the Hongge, Panzhihua and Baima intrusions have Fo values ranging from 63 to 83 mol.% (Wang et al., 2008b; Pang et al., 2009; Bai et al., 2012). This olivine did not crystallize from the most primitive magmas but from variably evolved magmas. In the Panzhihua and Baima intrusions, both concordant and discordant massive Fe-Ti oxide ore bodies are hosted in their lower parts where the majority of rocks are gabbroic in composition. Although the Hongge intrusion has ultramafic rocks in its lower part, the overall composition of the intrusion is not picritic. The intrusions in Panxi are relatively well preserved with clearly intrusive contacts with the country rocks. These features do not support the idea that they are parts of larger intrusions that contained Cr-rich titanomagnetite-bearing ultramafic rocks. Many ore-hosting intrusions are gabbroic in composition and formed from more evolved magmas. It is unlikely that ultramafic portions were tectonically removed, but it is possible that such evolved magmas underwent fractionation at depth before they were emplaced in shallow level chambers where the intrusions formed.

The host intrusions are rich in Fe and Ti, and thus must have crystallized from Fe-Ti rich magmas. It is difficult to envision how such dense, Fe-rich magmas could migrate from the mantle into shallow magma chambers. A more likely mechanism is that there were two stages of enrichment of Fe and Ti. The first stage was the melting of a Fe-Ti-rich mantle source and the second stage took place in a crustal magma chamber. The primitive picritic magmas were emplaced in a magma chamber where they fractionally crystallized and where the evolved, high-Fe liquids separated into Si-poor and Si-rich magmas. We note that a major feature of the oxide-bearing intrusions is their association with coeval syenitic plutons. Shellnutt et al. (2008, 2009a) favored the formation of these bi-modal components through normal fractionation. In their model, this fractionation enriched the magmas in Fe and Ti and explained the Daly gap between syenitic and gabbroic rocks.

On the other hand, it has been experimentally documented that a silicate liquid can evolve into an immiscible field (Fig. 18) (McBirney and Nakamura, 1974; Naslund, 1983; Hurai et al., 1998; Charlier and Grove, 2012). Experiments show that when the evolution trend reaches 52 to 55 wt.% SiO_2, the magma can separate into two immiscible liquids, one with 60–75 wt.% SiO_2 and 4–12 wt.% FeO^t, and the other with 30–50 wt.% SiO_2 and 18–32 wt.% FeO^t (Charlier and Grove, 2012). The oxide-bearing gabbros and associated syenites in the ELIP are compositionally comparable to the two immiscible melts (Shellnutt et al., 2009a, 2010b). Such immiscibility has also been convincingly demonstrated in the Skaergaard and Sept Iles intrusions through observations of coexisting melt inclusions hosted by apatite and plagioclase (Jakobsen et al., 2005, 2011; Charlier et al., 2011). The production of the two contrasting liquids has been proposed as an explanation for the compositional gap (i.e. Daly gap) observed in many ELIPs (e.g., Chayes, 1963; Shellnutt et al., 2009a; Charlier et al., 2011).

All the oxide-bearing intrusions of the ELIP and associated syenitic bodies plot in the fields of these two end-members (Fig. 18). Thus, it is possible that the mafic immiscible liquid formed the host gabbroic intrusions, whereas the Si-rich liquid formed the syenitic intrusions (Fig. 19). In this way, the mafic end-member would be further enriched in Fe-Ti metals, a primary requirement for the over-saturation of Fe and Ti in the magmas that eventually led to the separation of immiscible Fe-Ti oxide melts from the silicate magmas.

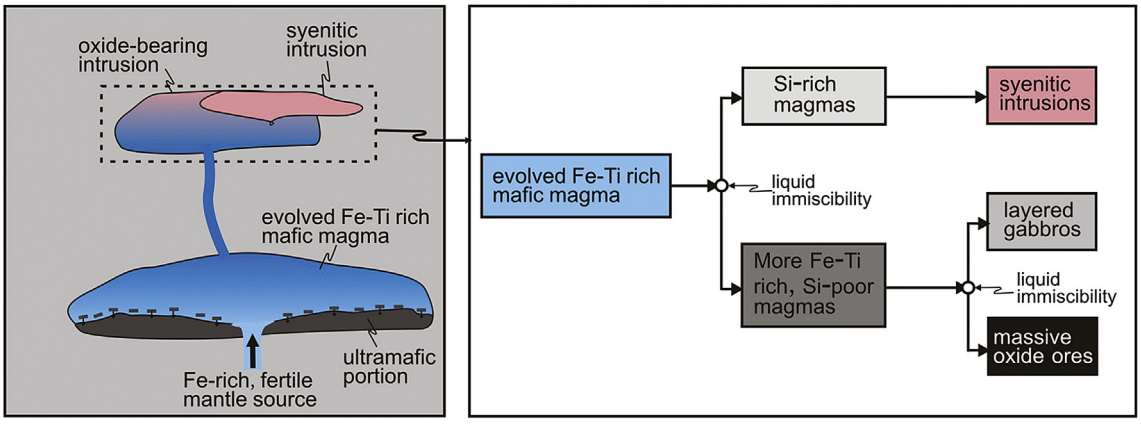

Figure 19. A schematic cartoon showing the formation model of the oxide deposits in the ELIP.

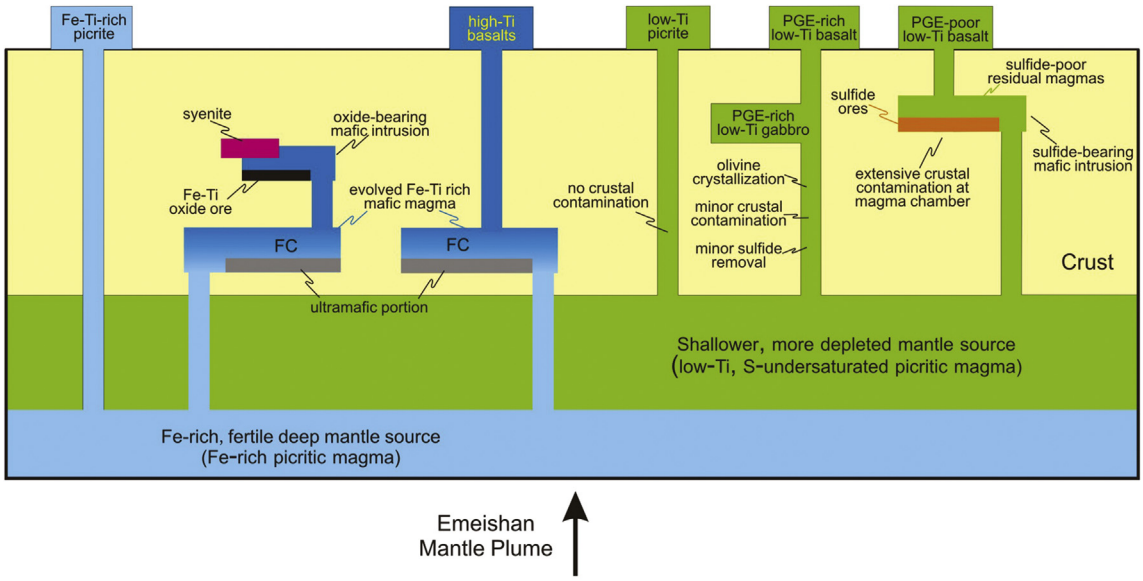

Figure 20. An integrated model for the ELIP magmatism that produced various rock types and associated deposits. High-Ti basalts experienced fractionation of olivine and chromite under S-undersaturated condition and are associated with the formation of oxide-bearing intrusions. Low-Ti mafic rocks formed by olivine dominated fractionation under S-undersaturated condition or sulfide saturation.

7.3.2. An integrated model of the mineralization of the ELIP

In our previous studies, we demonstrated that the mafic-ultramafic intrusions that host the Fe-Ti-V oxide deposits have much higher Ti, V, and Fe contents and lower Mg contents than those that host the Ni-Cu-(PGE) sulfide deposits (Zhou et al., 2008). The former magma series is rich in Ti and Fe and was produced from an enriched, OIB-type asthenospheric mantle source with EM-II characteristics. They erupted to the surface as Fe-rich picrites. If fractionation occurred at the depth, the evolved magmas could erupt as high-Ti basalts or be emplaced in shallower magma chambers as high-Ti gabbroic intrusions. Low pressure at shallow depth is considered more favorable for the separation of immiscible silicate liquids (Charlier et al., 2011). The evolved magma may enter the immiscible liquid fields to form both oxide-bearing mafic intrusions and syenitic plutons (Fig. 20). This model explains well the association of both oxide-bearing mafic intrusions and syenite bodies (Fig. 1).

On the other hand, the low-Ti picrites described in Hanski et al. (2004, 2010) may represent more primitive magmas that are considered to have derived from lithospheric mantle. The low-Ti basalts in the ELIP are highly evolved from such low-Ti picritic magmas and have Sr-Nd isotopic compositions indicative of extensive fractionation and crustal contamination (AFC) at a shallower depth (Wang et al., 2007).

Both the high-Ti and low-Ti series of rocks are widely distributed in the province. Their distributions are not related to the domal structure of the ELIP; i.e. the two types occur both in the central and peripheral parts of the dome. Related sulfide deposits are hosted in sills or dykes mainly in Devonian and Carboniferous strata in the Yangliuping area to the north and the Jinbaoshan area to the south. In the Jinping-Songda region, the southeastern ELIP, the Baimazhai sulfide deposit is hosted in Silurian strata and the Ban Phuc deposit of northern Vietnam in Devonian strata. Oxide-bearing intrusions are relatively large and mostly hosted in Sinian strata and were thought to be restricted in the Panxi region. We demonstrate that both the Anyi and Mianhuadi deposits have mineralization styles and geological settings similar to those in the Panxi area. In the Panxi region, both types of ore deposits co-exist but most likely they were emplaced at different depths. The eastern part of the ELIP is largely covered by Permian and Triassic strata so that ELIP-related intrusions and associated deposits are not exposed. In the Funing area, where the Devonian strata comprise the core of a major anticline, spatially associated oxide and sulfide-bearing intrusions are thought to have been derived from high-Ti and low-Ti magma series, respectively (Wang et al., 2011). Thus, the structure of the Emeishan mantle plume does not control the distribution of ELIP-related intrusions nor ore deposits. Our study suggests that ELIP-related oxide deposits may also occur elsewhere, wherever large intrusions are exposed by major faults.

8. Conclusions

Major Fe-Ti oxide deposits in the Panxi region are hosted in the lower parts of the layered intrusions. This type of deposit is not restricted to this region but examples such as the Anyi and Mianhuadi deposits occur farther to the south and southeast, near the border between Vietnam and China. The deposits are either discordant or conformable bodies with massive or disseminated ores. Net-textured ores are also present in some of these deposits. The host intrusions were derived from highly evolved gabbroic magmas that formed from Fe-picritic magmas after separation of an immiscible syenitic liquid. Magnetite ores formed from Fe-Ti-rich oxide melts that also were immiscible in gabbroic magmas.

Acknowledgments

This study is supported by the Research Grant Council of Hong Kong (HKU707012P) to MFZ, from a Chinese National “973” project (2011CB808903), and a “CAS Hundred Talents” project under Chinese Academy of Sciences to CYW, and South African National Science Foundation Grant SA/China Project 67220 to SP and MFZ. We thank several former PhD students at HKU who worked on various projects in the Panxi region, and Ma Yuxiao from Chengdu University of Science and Technology and geologists from the local mines for helping us with various matters. The study has benefited from collaboration with Nick T. Arndt who also provided details comments for this manuscript. We would express our thanks to Yigang Xu and two anonymous referees for thoughtful reviews.

Appendix B. Supplementary data

Supplementary data related to this article can be found at http://dx.doi.org/10.1016/j.gsf.2013.04.006.

References

Ali, J.R., Thompson, G.M., Zhou, M.-F., Song, X., 2005. Emeishan large igneous province, SW China. Lithos 79, 475–489.

Bai, Z.-J., Zhong, H., Naldrett, A.J., Zhu, W.-G., Xu, G.-W., 2012. Whole-rock and mineral composition constraints on the genesis of the giant Hongge Fe-Ti-V oxide deposit in the Emeishan large igneous province, southwest China. Economic Geology 107, 507–524.

Bateman, A.M., 1951. The formation of late magmatic ores. Economic Geology 46, 404–426.

Carmichael, I.S.E., 1967. The iron-titanium oxides of salic volcanic rocks and their associated ferromagnesian silicates. Contributions to MineralOgy and Petrology 14, 36–64.

Cawthorn, R.G., Molyneux, T.G., 1986. The vanadiferous magnetite deposits of the Bushveld Complex. In: Anhaeusser, C.R., Maske, S. (Eds.), Mineral Deposits of Southern Africa. Geological Society of South Africa, Juhannesburg, pp. 1251–1266.

Cawthorn, R.G., 1996. Layered Intrusions. Elsevier, Amsterdam, 531pp.

Cawthorn, R.G., Spies, L., 2003. Plagioclase content of cyclic units in the Bushveld Complex, South Africa. Contributions to Mineralogy and Petrology 145, 47–60.

Charlier, B., Namur, O., Toplis, M.J., Schiano, P., Cluzel, N., Higgins, M.D., Vander Auwera, J., 2011. Large-scale silicate liquid immiscibility during differentiation of tholeiitic basalt to granite and the origin of the Daly gap. Geology 39, 907–910.

Chayes, F., 1963. Relative abundance of intermediate members of the oceanic basalt-trachyte association. Journal of Geophysical Research 68, 1519–1534.

Charlier, B., Grove, T.L., 2012. Experiments on liquid immiscibility along tholeiitic liquid lines of descent. Contributions to Mineralogy and Petrology 164, 27–44.

Chung, S.L., Jahn, B.M., 1995. Plume-lithosphere interaction in generation of the Emeishan flood basalts at the Permian–Triassic boundary. Geology 23, 889–892.

Chung, S.L., Jahn, B.M., Wu, G., Lo, C.H., Cong, B., 1998. The Emeishan flood basalt in SW China: a mantle plume initiation model and its connection with continental breakup and mass extinction at the Permian-Triassic boundary. Mantle Dynamics and Plate Interactions in East Asia, Geodynamics Series 27, 47–58.

Duchesne, J.C., 1999. Fe–Ti deposits in Rogaland anorthosites (South Norway): geochemical characteristics and problems of interpretation. Mineralium Deposita 34, 182–198.

Eales, H.V., Cawthorn, R.G., 1996. The Bushveld complex. In: Cawthorn, R.G. (Ed.), Layered Intrusions. Elsevier, Amsterdam, pp. 181–232.

Gai, C.K., 2010. Geological features and ore genesis of the Fe-Ti-V oxide deposits in the Jinping area. Mineral Deposits 29 (Suppl.), 860–862 (in Chinese).

Ganino, C., Arndt, N.T., Zhou, M.F., Gaillard, F., Chauvel, C., 2008. Interaction of magma with sedimentary wall rock and magnetite ore genesis in the Panzhihua mafic intrusion, SW China. Mineralium Deposita 43, 677–694.

Ganino, C., Arndt, N.T., Chauvel, C., Jean, A., Athurion, C., 2013. Melting of carbonate wall rocks and formation of the heterogeneous aureole of the Panzhihua intrusion, China. Geoscience Frontiers 4, 535–546.

Hanski, E., Walker, R.J., Huhma, H., Polyakov, G.V., Balykin, P.A., Hoa, T.T., Phuong, N.T., 2004. Origin of the Permian–Triassic komatiites, northwestern Vietnam. Contributions to Mineralogy and Petrology 147, 453–469.

Hanski, E., Kamenetsky, V.S., Luo, Z.,-Y., Xu, Y.-G., Kuzmin, D.V., 2010. Primitive magmas in the Emeishan Large Igneous Province, southwestern China and northern Vietnam. Lithos 119, 75–90.

He, B., Xu, Y.G., Chung, S.L., Xiao, L., Wang, Y.M., 2003. Sedimentary evidence for a rapid, kilometer scale crustal doming prior to the eruption of the Emeishan flood basalts. Earth and Planetary Science Letters 213, 391–405.

He, B., Xu, Y.G., Huang, X.L., Luo, Z.Y., Shi, Y.R., Yang, Q.J., Yu, S.Y., 2007. Age and duration of the Emeishan flood volcanism, SW China: geochemistry and SHRIMP zircon U-Pb dating of silicic ignimbrites, post-volcanic Xuanwei Formation and clay tuff at the Chaotian section. Earth and Planetary Science Letters 225, 306–323.

He, B., Xu, Y.G., Guan, J.P., Zhong, Y.T., 2010. Paleokarst on the top of the Maokou Formation: further evidence for domal crustal uplift prior to the Emeishan flood volcanism. Lithos 119, 1–9.

Higgins, M.D., 2005. A new model for the structure of the Sept Iles Intrusive suite, Canada. Lithos 83, 199–213.

Hou, T., Zhang, Z.C., Ye, X., Encarnacion, J., Reichow, M.K., 2011. Noble gas isotopic systematics of FeeTieV oxide ore-related mafic-ultramafic layered intrusions in the Panxi area, China: the role of recycled oceanic crust in their petrogenesis. Geochimica et Cosmochimica Acta 75, 6727–6741.

Hou, T., Zhang, Z.C., Pirajno, F., 2012. A new metallogenic model of the Panzhihua giant V-Ti-iron oxide deposit (Emeishan Large Igneous Province) based on high-Mg olivine-bearing wehrlite and new field evidence. International Geology Review 54, 1721–1745.

Howarth, G.H., Prevec, S.A., Zhou, M.-F., 2013. Timing of Ti-magnetite crystallisation and silicate disequilibrium at the Panzhihua Mafic Layered Intrusion: implications for ore forming processes. Lithos. http://dx.doi.org/10.1016/j.lithos.2013.02.020.

Hurai, V., Simon, K., Wiechert, U., Hoefs, J., Konecny, P., Huraiova, M., Pironon, J., Lipka, J., 1998. Immiscible separation of metalliferous Fe/Ti-oxide melts from fractionating alkali basalt: P-T-fO_2 conditions and two-liquid elemental partitioning. Contributions to Mineralogy and Petrology 13, 12–19.

Irvine, T.N., 1977. Origin of chromitite layers in Muskox intrusion and other stratiform intrusions—a new interpretation. Geology 5, 273–277.

Jakobsen, J.K., Veksler, I.V., Tegner, C., Brooks, C.K., 2005. Immiscible iron-and silica-rich melts in basalt petrogenesis documented in the Skaergaard intrusion. Geology 33, 885–888.

Jakobsen, J.K., Veksler, I.V., Tegner, C., Brooks, C.K., 2011. Crystallization of the Skaergaard intrusion from an emulsion of immiscible iron- and silica-rich liquids: evidence from melt inclusions in plagioclase. Journal of Petrology 52, 345–373.

Kolker, A., 1982. Mineralogy and geochemistry of Fe-Ti oxide and apatite (nelsonite) deposits and evaluation of the liquid immiscibility hypothesis. Economic Geology 77, 1146–1158.

Lee, C.A., 1996. A review of mineralization in the Bushveld complex and some other layered mafic intrusions. In: Cawthorn, R.G. (Ed.), Layered Intrusions. Elsevier, Amsterdam, pp. 103–146.

Luo, T.X., 2007. The Maanshan titanomagnetite deposit in Jinping, Yunnan. Yunnan Geology 26, 124–128 (in Chinese with English abstract).

Ma, Y., Ji, X.T., Li, J.C., Huang, M., Kan, Z.Z., 2003. Mineral Resources of the Panzhihua Region. Sichuan Science and Technology Press, Chengdu, 275pp. (in Chinese).

McBirney, A.R., Nakamura, Y., 1974. Immiscibility in late-stage magmas of the Skaergaard intrusion. Carnegie Institution of Washington Year Book 73, 348–352.

McBirney, A.R., 1996. The Skaergaard intrusion. In: Cawthorn, R.G. (Ed.), Layered Intrusions. Elsevier, Amsterdam, pp. 147–180.

Naslund, H.R., 1983. The effect of oxygen fugacity on liquid immiscibility in iron-bearing silicate melts. American Journal of Science 283, 1034–1059.

Pang, K.-N., Zhou, M.-F., Lindsley, D.H., Zhao, D., Malpas, J., 2008a. Origin of Fe-Ti oxide ores in mafic intrusions: evidence from the Panzhihua intrusion. Journal of Petrology 49, 295–313.

Pang, K.N., Li, C., Zhou, M.-F., Ripley, E.M., 2008b. Abundant Fe-Ti oxide inclusions in olivine from the Panzhihua and Hongge layered intrusions, SW China: evidence for early saturation of Fe-Ti oxides in ferrobasaltic magma. Contributions to Mineralogy and Petrology 156, 307–321.

Pang, K.N., Li, C., Zhou, M.-F., Ripley, E.M., 2009. Mineral compositional constraints on petrogenesis and oxide ore genesis of the late Permian Panzhihua layered gabbroic intrusion, SW China. Lithos 110, 199–214.

Pang, K.N., Zhou, M.-F., Qi, L., Shellnutt, J.G., Wang, C.Y., Zhao, D.G., 2010. Flood basalt-related Fe–Ti oxide deposits in the Emeishan large igneous province, SW China. Lithos 119, 123–136.

Panxi Geological Team, 1987. Ore Formation and Geology of the Hongge Fe-Ti-V Oxide Deposit in Sichuan. Geological Publishing House, Beijing.

Peng, H.B., 2009. The metallogenetic conditions of Dapo ore block of Mianhuadi titanomagnetite deposit in Jinping. Yunnan Geology 28, 143–147 (in Chinese with English abstract).

Pecher, A., Arndt, N., Jean, A., Bauville, A., Ganino, C., Athurion, C., 2013. Structurenof the Panzhihua intrusion and its Fe-Ti-V deposit, China. Geoscience Frontiers 4, 571–581.

Philpotts, A.R., 1967. Origin of certain iron–titanium oxide and apatite rocks. Economic Geology 62, 303–315.

Philpotts, A.R., 1976. Silicate liquid immiscibility: its probable extent and petrogenetic significance. American Journal of Science 276, 1147–1177.

Philpotts, A.R., 1982. Compositions of immiscible liquids in volcanic rocks. Contributions to Mineralogy and Petrology 80, 201–218.

Qi, L., Zhou, M.-F., 2008. Platinum-group elemental and Sr-Nd-Os isotopic geochemistry of Permian Emeishan flood basalts in Guizhou Province, SW China. Chemical Geology 248, 83–103.

Qi, L., Wang, C.Y., Zhou, M.F., 2008. Controls on the PGE distribution of Permian Emeishan alkaline and peralkaline volcanic rocks in Longzhoushan, Sichuan Province, SW China. Lithos 106, 222–236.

Reynolds, I.M., 1985. Contrasted mineralogy and textural relationships in the uppermost titaniferous magnetite layers of the Bushveld complex in the Bierkraal area north of Rustenburg. Economic Geology 80, 1027–1048.

Ripley, E.M., Severson, M.J., Hauck, S.A., 1998. Evidence for sulfide and Fe–Ti–P-rich liquid immiscibility in the Duluth complex, Minnesota. Economic Geology 93, 1052–1062.

Shellnutt, J.G., Zhou, M.-F., 2007. Permian peralkaline, peraluminous and metaluminous A-type granites in the Panxi district, SW China: their relationship to the Emeishan mantle plume. Chemical Geology 243, 286–316.

Shellnutt, J.G., Zhou, M.-F., 2008. Permian, rifting related fayalite syenite in the Panxi region, SW China. Lithos 101, 54–73.

Shellnutt, J.G., Zhou, M.-F., Yan, D.P., Wang, Y.B., 2008. Longevity of the Permian Emeishan mantle plume (SW China): 1 Ma, 8 Ma or 18 Ma? Geological Magazine 145, 373–388.

Shellnutt, J.G., Zhou, M.-F., Zellmer, G., 2009a. The role of Fe-Ti oxide crystallization in the formation of A-type granitoids with implications for the Daly gap: an example from the Permian Baima igneous complex, SW China. Chemical Geology 259, 204–217.

Shellnutt, J.G., Wang, C.Y., Zhou, M.-F., Yang, Y.H., 2009b. Zircon Lu-Hf isotopic compositions of metaluminous and peralkaline A-type granitic plutons of the Emeishan large igneous province (SW China): constraints on the mantle source. Journal of Asian Earth Sciences 35, 45–55.

Shellnutt, J.G., Zhou, M.-F., Chung, S.L., 2010a. The Emeishan large igneous province: advances in the stratigraphic correlations and petrogenetic and metallogenic models. Lithos 119, ix–x.
Shellnutt, J.G., Jahn, B.-M., Dostal, J., 2010b. Elemental and Sr-Nd isotope geochemistry of microgranular enclaves from peralkaline A-type granitic plutons of the Emeishan large igneous province, SW China. Lithos 119, 34–46.
Shellnutt, J.G., Wang, K.-L., Zellmer, G.F., Iizuka, Y., Jahn, B.-M., Pang, K.-N., Qi, L., Zhou, M.F., 2011. Three Fe-Ti oxide ore-bearing gabbro-granitoid complexes in the Panxi region of the Permian Emeishan large igneous province, SW China. American Journal of Science 311, 773–812.
Shellnutt, J.G., Pang, K.N., 2012. Petrogenetic implications of mineral chemical data for the Permian Baima igneous complex, SW China. Mineralogy and Petrology 106, 75–88.
Shellnutt, J.G., Denyszyn, S.W., Mundil, R., 2012. Precise age determination of mafic and felsic intrusive rocks from the Permian Emeishan large igneous province (SW China). Gondwana Research 2012, 118–126.
Sisson, T.W., Grove, T.L., 1993. Experimental investigations of the role of H2O in calc-alkaline differentiation and subduction zone magmatism. Contributions to Mineralogy and Petrology 113, 143–166.
Song, X.-Y., Zhou, M.-F., Wang, Y.-L., Zhang, C., Cao, Z., Li, Y., 2001. Geochemical constrains on the mantle source of the Upper Permian Emeishan continental flood basalts, SW China. International Geology Review 43, 213–225.
Song, X.-Y., Zhou, M.-F., Cao, Z.M., Sun, M., Wang, Y.L., 2003. Ni-Cu-(PGE) magmatic sulfide deposits in the Yangliuping area, Permian Emeishan Igneous province, SW China. Mineralium Deposita 38, 831–843.
Song, X.-Y., 2004. Geochemistry of Permian Flood Basalts and Related Ni-Cu-(PGE) Sulfide-bearing Sills in Yangliuping, Sichuan Province, China. Ph.D thesis of the University of Hong Kong.
Song, X.-Y., Zhou, M.-F., Cao, Z.M., Robinson, P.T., 2004. Late permian rifting of the South China Craton caused by the Emeishan mantle plume? Journal of the Geological Society 161, 773–781.
Song, X.-Y., Zhou, M.-F., Keays, R.R., Cao, Z., Sun, M., Qi, L., 2006. Geochemistry of the Emeishan flood basalts at Yangliuping, Sichuan, SW China: implications for sulfide segregation. Contributions to Mineralogy and Petrology 152, 53–74.
Song, X.-Y., Zhou, M.-F., Tao, Y., Xiao, J.F., 2008. Controls on the metal compositions of magmatic sulfide deposits in the Emeishan large igneous province, SW China. Chemical Geology 253, 38–49.
Tao, Y., Li, C., Hu, R., Ripley, E.M., Du, A., Zhong, H., 2007. Petrogenesis of the Pt–Pd mineralized Jinbaoshan ultramafic intrusion in the Permian Emeishan Large Igneous Province, SW China. Contributions to Mineralogy and Petrology 153, 321–337.
Tao, Y., Ma, Y.S., Miao, L.C., Zhu, F.L., 2009. SHRIMP U-Pb zircon age of the Jinbaoshan ultramafic intrusion, Yunnan province, SW China. Chinese Science Bulletin 54, 168–172.
Tao, Y., Li, C., Hu, R., Qi, L., Qu, W., Du, A., 2010. Re–Os isotopic constraints on the genesis of the Limahe Ni–Cu deposit in the Emeishan large igneous province, SW China. Lithos 119, 137–146.
Wager, L.R., Brown, G.M., 1968. Layered Igneous Rocks. Oliver and Boyd, Edinburgh, 588pp.
Wang, C.Y., Zhou, M.-F., Zhao, D., 2005. Mineral chemistry of chromite from the Permian Jinbaoshan Pt-Pd-sulphide-bearing ultramafic intrusion in SW China with petrogenetic implications. Lithos 83, 47–66.
Wang, C.Y., Zhou, M.-F., 2006. Genesis of the Permian Baimazhai magmatic Ni-Cu-(PGE) sulfide deposit, Yunnan, SW China. Mineralium Deposita 41, 771–783.
Wang, C.Y., Zhou, M.-F., Keays, R.R., 2006. Geochemical constraints on the origin of the Permian Baimazhai mafic-ultramafic intrusion, SW China. Contributions to Mineralogy and Petrology 152, 309–321.
Wang, C.Y., Zhou, M.-F., Qi, L., 2007. Permian flood basalts and mafic intrusions in the Jinping (SW China) Song Da (northern Vietnam) district: mantle sources, crustal contamination and sulfide segregation. Chemical Geology 243, 317–343.
Wang, C.Y., Prichard, H.M., Zhou, M.-F., Fisher, P.C., 2008a. Platinum-group minerals from the Jinbaoshan Pd–Pt deposit, SW China: evidence for magmatic origin and hydrothermal alteration. Mineralium Deposita 43, 791–803.
Wang, C.Y., Zhou, M.-F., Zhao, D.G., 2008b. Fe-Ti-Cr oxides from the Permian Xinjie mafic-ultramafic layered intrusion in the Emeishan large igneous province, SW China: crystallization from Fe- and Ti-rich basaltic magmas. Lithos 102, 198–217.
Wang, C.Y., Zhou, M.-F., Qi, L., 2010. Origin of extremely PGE-rich mafic magma system: an example from the Jinbaoshan ultramafic sill, Emeishan large igneous province, SW China. Lithos 119, 147–161.
Wang, C.Y., Zhou, M.-F., Qi, L., 2011. Chalcophile element geochemistry and petrogenesis of high-Ti and low-Ti magmas in the Permian Emeishan large igneous province, SW China. Contributions to Mineralogy and Petrology 161, 237–254.
Wang, C.Y., Zhou, M.-F., Sun, Y., Arndt, N.T., 2012. Differentiation, crustal contamination and emplacement of magmas in formation of the Nantianwan mafic intrusion of the ~ 260 Ma Emeishan large igneous province, SW China. Contributions to Mineralogy and Petrology 164, 281–301.
Wang, C.Y., Zhou, M.-F., 2013. New textural and mineralogical constraints on the origin of the Hongge Fe-Ti-V oxide deposit, SW China. Mineralium Deposita. http://dx.doi.org/10.1007/s00126-013-0457-4.
Xing, C.M., Wang, C.Y., Zhang, M., 2012. Volatile and C-H-O isotopic compositions of giant Fe-Ti-V oxide deposits in the Panxi region and their implications for the source of volatiles and the origin of Fe-Ti oxide ores. Science China Earth China. http://dx.doi.org/10.1007/s11430-012-4468-2.
Xu, Y.G., Chung, S.L., Jahn, B.M., Wu, G., 2001. Petrologic and geochemical constraints on the petrogenesis of Permian–Triassic Emeishan flood basalts in southwestern China. Lithos 58, 145–168.
Xu, Y.G., He, B., Chung, S.L., Menzies, M.A., Frey, F.A., 2004. Geologic, geochemical, and geophysical consequences of plume involvement in the Emeishan flood-basalt province. Geology 32, 917–920.
Xu, Y.-G., Luo, Z.-Y., Huang, X.-L., He, B., Xiao, L., Xie, L.-W., Shi, Y.-R., 2008. Zircon U-Pb and Hf isotope constraints on crustal melting associated with the Emeishan mantle plume. Geochimica et Cosmochimica Acta 72, 3084–3104.
Yao, P.H., Wang, K.N., Du, C.L., Lin, Z.T., Song, X., 1993. Records of China's Iron Ore Deposits. Metallurgical Industry Press, Beijing, China, pp. 633–649. (in Chinese).
Zhang, Y.X., Luo, Y.N., Yang, C.X., 1988. The Panxi Rift (in Chinese). Geological Publishing House, Beijing, pp. 1–325.
Zhang, M., Hu, P., Niu, Y., Su, S., 2007. Chemical and stable isotopic constraints on the nature and origin of volatiles in the sub-continental lithospheric mantle beneath China. Lithos 96, 55–66.
Zhang, M., Niu, Y., Hu, P., 2009. Volatiles in the mantle lithosphere: modes of occurrence and chemical compositions. In: Anderson, J.E., Coates, R.W. (Eds.), The Lithosphere: Geochemistry, Geology and Geophysics. Nova Science Publishers Inc, New York, pp. 171–212.
Zhang, Z.C., Mahoney, J.J., Mao, J.W., Wang, F.S., 2006. Geochemistry of picritic and associated basalt flow of the western Emeishan flood basalt province, China. Journal of Petrology 47, 1997–2019.
Zhang, Z.C., Zhi, X.C., Chen, L., Saunders, A.D., Reichow, M.K., 2008. Re-Os isotopic compositions of picrites from the Emeishan flood basalt province, China. Earth and Planetary Science Letters 276, 30–39.
Zhang, Z.C., Mao, J.W., Saunders, A.D., Ai, Y., Li, Y., Zhao, L., 2009. Petrogenetic modeling of three maficeultramafic layered intrusions in the Emeishan large igneous province, SW China, based on isotopic and bulk chemical constraints. Lithos 113, 369–392.
Zhang, Z.Q., Lu, J.R., Tang, S.H., 1999. Sm-Nd ages of the Panxi layered basic-ultrabasic intrusions in Sichuan. Acta Geologica Sinica 73, 263–271 (in Chinese).
Zhong, H., Zhou, X.H., Zhou, M.-F., Sun, M., Liu, B.G., 2002. Platinum-group element geochemistry of the Hongge Fe-V-Ti deposit in the Pan-Xi area, southwestern China. Mineralium Deposita 37, 226–239.
Zhong, H., Yao, Y., Hu, S.F., Zhou, X.H., Liu, B.G., Sun, M., Zhou, M.-F., Viljoen, M.J., 2003. Trace-element and Sr-Nd isotopic geochemistry of the PGE-bearing Hongge layered intrusion, southwestern China. International Geology Review 45, 371–382.
Zhong, H., Hu, R.Z., Wilson, A.H., Zhu, W.G., 2005. Review of the link between the Hongge layered intrusion and Emeishan flood basalts, southwest China. International Geology Review 47, 971–985.
Zhong, H., Zhu, W.G., 2006. Geochronology of layered mafic intrusions from the Pan–Xi area in the Emeishan large igneous province, SW China. Mineralium Deposita 41 (6), 599–606.
Zhong, H., Zhu, W.-G., Chu, Z.-Y., He, D.-F., Song, X.-Y., 2007. Shrimp U-Pb zircon geochronology, geochemistry, and Nd-Sr isotopic study of contrasting granites in the Emeishan large igneous province, SW China. Chemical Geology 236, 112–133.
Zhong, H., Zhu, W.-G., Hu, R.-Z., Xie, L.-W., He, D.-F., Liu, F., Chu, Z.-Y., 2009. Zircon U-Pb age and Sr-Nd-Hf isotope geochemistry of the Panzhihua A-type syenitic intrusion in the Emeishan large igneous province, southwest China and implications for growth of juvenile crust. Lithos 110, 109–128.
Zhong, H., Campbell, I.H., Zhu, W.-G., Allen, C.M., Hu, R.Z., Xie, L.W., He, D.F., 2011. Timing and source constraints on the relationship between mafic and felsic intrusions in the Emeishan large igneous province. Geochimica et Cosmochimica Acta 75, 137–1395.
Zhou, M.-F., Malpas, J., Song, X., Kennedy, A.K., Robinson, P.T., Sun, M., Lesher, C.M., Keays, R.R., 2002a. A temporal link between the Emeishan large igneous province (SW China) and the end-Guadalupian mass extinction. Earth and Planetary Science Letters 196, 113–122.
Zhou, M.-F., Yan, D.P., Kennedy, A.K., Li, Y.Q., Ding, J., 2002b. SHRIMP zircon geochronological and geochemical evidence for Neo-proterozoic arc-related magmatism along the western margin of the Yangtze Block, South China. Earth and Planetary Science Letters 196, 51–67.
Zhou, M.-F., Robinson, P.T., Lesher, C.M., Keays, R.R., Zhang, C.J., Malpas, J., 2005. Geochemistry, petrogenesis and metallogenesis of the Panzhihua gabbroic layered intrusion and associated Fe-Ti-V oxide deposits, Sichuan Province, SW China. Journal of Petrology 46, 2253–2280.
Zhou, M.-F., Zhao, J.H., Qi, L., Su, W.C., Hu, R.Z., 2006. Zircon U-Pb geochronology and elemental and Sr-Nd isotope geochemistry of Permian mafic rocks in the Funing area, SW China. Contributions to Mineralogy and Petrology 151, 1–19.
Zhou, M.-F., Arndt, N.T., Malpas, J., Wang, C.Y., Kennedy, A.K., 2008. Two magma series and associated ore deposit types in the Permian Emeishan Large Igneous Province, SW China. Lithos 103, 352–368.